

Warm Season Rainfall Variability over the U.S. Great Plains in Observations, NCEP and ERA-40 Reanalyses, and NCAR and NASA Atmospheric Model Simulations

ALFREDO RUIZ-BARRADAS

Department of Atmospheric and Oceanic Science, University of Maryland, College Park, College Park, Maryland

SUMANT NIGAM

Department of Atmospheric and Oceanic Science, and Earth System Science Interdisciplinary Center, University of Maryland, College Park, College Park, Maryland

(Manuscript received 11 March 2004, in final form 20 September 2004)

ABSTRACT

Interannual variability of Great Plains precipitation in the warm season months is analyzed using gridded observations, satellite-based precipitation estimates, NCEP reanalysis data and the 40-yr European Centre for Medium-Range Weather Forecasts (ECMWF) Re-Analysis (ERA-40) data, and the half-century-long NCAR Community Atmosphere Model (CAM3.0, version 3.0) and the National Aeronautics and Space Administration (NASA) Seasonal-to-Intraseasonal Prediction Project (NSIPP) atmospheric model simulations. Regional hydroclimate is the focus because of its immense societal impact and because the involved variability mechanisms are not well understood.

The Great Plains precipitation variability is represented rather differently, and only quasi realistically, in the reanalyses. NCEP has larger amplitude but less traction with observations in comparison with ERA-40. Model simulations exhibit more realistic amplitudes, which are between those of NCEP and ERA-40. The simulated variability is however *uncorrelated* with observations in both models, with monthly correlations smaller than 0.10 in all cases. An assessment of the regional atmosphere water balance is revealing: Stationary moisture flux convergence accounts for most of the Great Plains variability in ERA-40, but not in the NCEP reanalysis and model simulations; convergent fluxes generate less than half of the precipitation in the latter, while local evaporation does the rest in models.

Phenomenal evaporation in the models—up to 4 times larger than the highest observationally constrained estimate (NCEP's)—provides the bulk of the moisture for Great Plains precipitation variability; thus, precipitation recycling is very efficient in both models, perhaps too efficient.

Remote water sources contribute substantially to Great Plains hydroclimate variability in nature via fluxes. Getting the interaction pathways right is presently challenging for the models.

1. Introduction

Agriculture and water resources in the central and eastern United States are profoundly influenced by atmospheric circulation, precipitation, and streamflow in summer—the growing season. Circulation is an influential element of regional hydroclimate since moisture transports contribute substantially to local precipitation and also because circulation can influence the precipitation distribution by modulating the strength and/or position of storm tracks. Interest in the warm season's circulation and precipitation *variability* has greatly increased following the 1988 drought over much of the

continental United States and the Midwest floods during 1993. An improved understanding of the origin and development mechanisms of the regional- to continental-scale variability patterns will advance the accuracy of hydroclimate forecasts—an important objective of the U.S. global water cycle initiative (Hornberger et al. 2001).

Significant strides were recently made by showing the North American hydroclimate to be linked to El Niño–Southern Oscillation (ENSO) and Pacific decadal variability. Regional hydroclimate anomalies have also been attributed to the interaction of upstream flow anomalies and the Rockies, changes in summertime storm tracks, and anomalous antecedent soil moisture. An awareness of the potential mechanisms does not necessarily lead to improved simulations and predictions of variability, though. The relative importance of

Corresponding author address: Sumant Nigam, 3419 Computer and Space Sciences Bldg., University of Maryland, College Park, College Park, MD 20742-2425.
E-mail: nigam@atmos.umd.edu

these mechanisms in nature and the extent to which the key ones are represented in general circulation models (GCMs) will determine the simulation and prediction quality. Assessment efforts invariably begin with an examination of the structure of dynamical and thermodynamical interactions operative in nature and models (i.e., with the “how” rather than “why” questions). The key how questions—a subset of which is examined here—are as follows:

- How important are the relative contributions of local and remote water sources (e.g., evaporation and moisture fluxes, respectively) in North American precipitation variability? What is the extent of precipitation recycling?
- How large is the relative contribution of convective and stratiform (large-scale condensation) processes in warm season precipitation. Precipitation in mid-latitudes (e.g., the Great Plains region) is produced mostly in deep stratiform clouds (nimbostratus) that form in the mature phase of the mesoscale convective complexes, but the convective contribution can be significant in summer. Knowing the precipitation mix is important for regional circulation and radiation feedbacks since these processes are associated with substantially different heating profiles and cloud bases.
- How strong is the linkage between North American precipitation variability and the adjoining ocean basins, in particular, the moisture pathways for the Pacific connection. What is the nature of this linkage?
- How critical is the role of soil moisture in generation of hydroclimate variability? Is the feedback important only for the local amplitude or also for the large-scale pattern structure?

The regional expression of seasonal to interannual climate variability and global change has attracted a lot of attention recently, for both societal and scientific reasons: The economic value of regional hydroclimate predictions can, of course, be considerable. But the scientific value of regional simulations and predictions is no less important if the region is densely observed; model exercises in such regions facilitate model validation and development.

One such region is the U.S. Great Plains. As suggested by its name, the Great Plains region is devoid of the complex terrain found farther to the west and southwest. Simulation of Great Plains hydroclimate variability cannot thus be regarded as an onerous burden on numerical climate models having horizontal resolution of a few degrees of latitude and longitude. On the other hand, the Great Plains are located in the midlatitudes, where internally generated atmospheric

variability cannot be ignored, even during summer. Generating the right mix of internally generated and lower-boundary-forced variability can be challenging for models. Atmospheric general circulation models produce large-scale hydroclimate variability when forced by anomalous conditions in the adjoining ocean basins, but the resulting patterns are often unrealistic.

Stationary (monthly averaged) and transient (sub-monthly) moisture fluxes provide a key link between precipitation and the larger-scale circulation. The fluxes highlight subtle features of the flow that are crucial for moisture transports, as in the Great Plains low-level jet region. Investigation of the Pacific and Atlantic basin links with moisture fluxes can provide insight into the mechanisms generating low-frequency hydroclimate variability, especially if moisture flux convergence dominates evaporation in the regional atmospheric water balance. The insights may also help understand why state-of-the-art models are currently unable to simulate warm season hydroclimate variability.

The present study can be viewed as somewhat complementary to the earlier investigations of Nigam et al. (1999) and Barlow et al. (2001). Instead of analyzing the warm season hydroclimate linkages of recurrent Pacific SST variability, the present study examines, more directly, the linkages of Great Plains precipitation variability; the continental precipitation-centric analysis strategy is thus one distinction. A strong emphasis on the assessment of GCM simulations of North American hydroclimate *variability* is another, as is the analysis of linkage to the Atlantic basin. Extensive intercomparison of the National Centers for Environmental Prediction (NCEP) reanalysis and the 40-yr European Centre for Medium-Range Weather Forecasts (ECMWF) Re-Analysis (ERA-40), and an evaluation of their own quality in context of Great Plains precipitation, evaporation, and moisture flux variability is another distinctive aspect.¹ The present study makes a contribution to the North American Monsoon Experiment (NAME) subprogram on model intercomparison and development, the North American Monsoon Intercomparison Project (http://www.joss.ucar.edu/cgi-bin/name/namip/namip_quest).

Interannual variability of the Great Plains hydroclimate has been extensively studied from both observational and modeling analyses: Warm season anomalies have been linked with tropical Pacific SSTs (Trenberth

¹ The ERA-40 dataset was produced from a high-resolution global modeling system that was operational until 2002, whereas NCEP reanalysis was generated using a 1995 period system. ERA-40, thus, implicitly benefits from the improvements in models and data assimilation techniques realized in the intervening years.

et al. 1988; Trenberth and Guillemot 1996; Schubert et al. 2004), with North Pacific SST and diabatic heating anomalies (Ting and Wang 1997; Liu et al. 1998; Higgins et al. 1999; Nigam et al. 1999; Barlow et al. 2001), with anomalous upstream flow over the Rockies (Mo et al. 1995), with southerly anomalies from the Gulf of Mexico (Hu and Feng 2001), with midlatitude storm track variations (Trenberth and Guillemot 1996), and with anomalous antecedent soil moisture (Namias 1991; Bell and Janowiak 1995; Koster et al. 2003). The linkage of Pacific SST variability with U.S. hydroclimate is not very strong: The largest station regressions for ENSO or the decadal modes typically explain only about one-quarter of the local monthly variance during June–August (Barlow et al. 2001). Although significant, this alone cannot be the basis for potential predictability of the warm season hydroclimate. Clearly, other linkages must be investigated—among them, the connection to Atlantic SSTs, which Namias (1966) considered important, especially for the eastern part of the continent. The influence of the North Atlantic Oscillation on U.S. warm season precipitation and circulation is examined in this study.

The nearly 50-yr-long atmospheric model simulations analyzed in this study were generated at the climate modeling centers from integrations with specified (observed) lower boundary conditions (SST, sea ice), much as those routinely produced for the Atmospheric Model Intercomparison Project (AMIP) (Gates 1999).² Simulated and observed circulation and hydroclimate anomalies can be expected to be in some agreement in *each* summer if the SST-forced variability component was dominant (and the model simulation realistic); otherwise, the two anomalies can be compared only in some aggregate sense: For example, precipitation regressions on a SST variability index (or SST regressions on a precipitation index) can be compared; the regressions filter out the internally generated (and uncorrelated) fluctuations.³

The datasets used in hydroclimate validation are briefly described in section 2. The Great Plains precipitation variability in the gridded station datasets, NCEP

and ERA-40 reanalyses, and two AMIP model simulations are discussed in section 3, while the accompanying spatial patterns of rainfall, stationary and transient moisture fluxes, and evaporation variability are targeted in section 4. The SST linkages of Great Plains precipitation in observations and model simulations are also shown in this section. The recurrent patterns of warm season SST and lower-tropospheric circulation (700-hPa geopotential) variability having bearing on the Great Plains hydroclimate are objectively identified in section 5. Discussions and concluding remarks follow in section 6.

2. Datasets

Several observational datasets are used in model assessments. These include the two atmospheric reanalysis products: from NCEP–National Center for Atmospheric Research (NCAR) (Kalnay et al. 1996) and from ERA-40 (details online at <http://www.ecmwf.int/products/data/archive/descriptions/e4/>). Precipitation is of key interest in this study and, fortunately, it has been directly and independently measured at ground stations for some time, albeit with modest spatial and temporal resolution. The gridded precipitation observations used in this analysis come from NCEP’s Climate Prediction Center (CPC) and the University of East Anglia (UEA) (Hulme 1999). Two CPC products are used: the first is a retrospective analysis of daily station precipitation over the United States and Mexico (more information available online at <http://www.cpc.ncep.noaa.gov/products/precip/realtime/retro.html>; hereafter, referred as the U.S.–Mexico station dataset) while the second is a satellite and rain gauge–based Merged Analysis of Precipitation (CMAP-2; Xie and Arkin 1997). The Xie–Arkin dataset is short, beginning in January 1979, but valuable for ascertaining the impact of spotty spatial coverage of the station-based datasets. The SST links are obtained using the Hadley Centre’s Sea Ice and SST analysis (the HadISST data: Rayner et al. 2003). Spatial resolution of the datasets differ, and is generally noted in the title line of the display panels.

The nearly 50-yr-long (1950–98) AMIP integrations of the National Center for Atmospheric Research Community Atmospheric Model (CAM3.0, version 3.0) were produced using Hurrell’s SST analysis (J. Hurrell 2003, personal communication); the SSTs were obtained by merging HadISSTs with version 2 of the National Oceanic and Atmospheric Administration (NOAA) optimum interpolation (OI.v2) SSTs (Reynolds et al. 2002). The AMIP simulations with National Aeronautics and Space Administration (NASA) Seasonal-to-Interannual Prediction Project (NSIPP) atmospheric model were produced using the Hadley Cen-

² Specifying SST in the middle and high latitudes is, perhaps, unnecessary since SST variability is strongly influenced by the overlying atmosphere here. It is presently unclear if allowing SST evolution in the extratropics through mixed-layer thermodynamics, for example, leads to improved simulation in local and remote regions.

³ Very often, an ensemble of AMIP simulations is generated with the hope that the ensemble mean will directly reveal the SST-forced signal, and it does, without additional compositing or regression analysis. An ensemble mean allows for apportioning of *each* summer’s anomaly into SST-forced and internally generated components, but it does not contribute to additional model validation.

tre's Global Sea Ice and SST dataset (GISST: Rayner et al. 1996; the predecessor of HadISST) for the 1949–81 period and Reynolds OI SSTs thereafter. The SST dataset differences (and their impact) are however anticipated to be insignificant in comparison with the model structure and parameterization differences. An eight-member ensemble of AMIP simulations was generated with the NSIPP model using slightly different initial conditions; the fifth ensemble member and the ensemble mean are analyzed here; the first ensemble member and the five-member ensemble mean are analyzed in the case of CAM3.0. Note, the analyzed models are components of the current NCAR and NSIPP climate system models, respectively.

The contribution of local and remote water sources in Great Plains precipitation variability is examined in observations and model simulations using observationally constrained evaporation estimates. In addition to those provided by the two reanalyses, evaporation estimates generated at NOAA's CPC (Huang et al. 1996) and the Center for Ocean–Land–Atmosphere Studies (COLA) (Dirmeyer and Tan 2001) are also used in model assessments; the monthly, gridded estimates are available for several recent decades at near-degree-scale resolution.

Interannual variability is analyzed using monthly anomalies, calculated with respect to the 1950–98 monthly climatology whenever possible; the attention is on the northern warm season months of June–August (JJA).

3. Great Plains precipitation index

a. Precipitation variability

The extent of interannual variability in warm season precipitation is examined in Fig. 1 by displaying the standard deviation (SD) of *monthly* precipitation anomalies in observations (Figs. 1a–c) and reanalysis datasets (Figs. 1d,e) over North America. The two station datasets are similar over the United States, with a local maximum in interannual precipitation variability over the Great Plains region. The UEA data exhibit marginally greater variability in the coastal regions, despite its coarseness; grid-averaged precipitation can, however, be influenced by orographic resolution in an unpredictable manner in coastal zones. The satellite-based Xie–Arkin precipitation has an interannual variability range that is similar to the surface-based records; the amplitude is a bit weaker, though, especially over the Great Plains where the maximum is now less than 1.5 mm day^{-1} . Comparison of the three standard deviations in the same 20-yr subperiod (1979–98) shows that weaker variability in Fig. 1c is not an artifact of the period differences; the discrepancy over Great Plains is,

if anything, greater now, with the U.S.–Mexico data exhibiting an amplitude in excess of 1.8 mm day^{-1} in places.

The depiction of warm season precipitation variability in the reanalysis datasets (Figs. 1d,e) is quasi realistic. Although the southeastern focus is captured in both, ERA-40 underestimates while NCEP overestimates the magnitude of interannual variability in the Ohio Valley and Great Plains regions; NCEP's tendency to overestimate precipitation variability has been noted before (e.g., Janowiak et al. 1998). The higher resolution of ERA-40 is evident from the presence of small-scale features in Fig. 1e and from the very large amplitudes over portions of Mexico and Central America; also evident is a spurious feature over Colorado and New Mexico.

Warm season precipitation variability in the AMIP simulations is shown in Fig. 2. The simulations are in reasonable agreement among themselves and with observations over the western United States, but some differences are evident in the eastern half. The local maximum over the Great Plains is somewhat diffuse but otherwise well positioned in the CAM simulation. The same feature in the NSIPP simulation is too strong ($\approx 2.1 \text{ mm day}^{-1}$) and westward shifted in comparison with observations. The Gulf Coast focus is also missing in the CAM simulation. It is noteworthy that the interannual variability of Great Plains precipitation is large, being 30%–50% of the climatology in most places.

b. Index definition

An index is often used to describe the temporal variability of a spatially coherent region. One such region is marked in the Fig. 1 panels. The square box (35° – 45° N, 100° – 90° W) evidently encompasses the region exhibiting a local maximum in observed precipitation variability (Figs. 1a–c). The boxed region includes the states of South Dakota, Minnesota, Wisconsin, Nebraska, Iowa, Illinois, Kansas, Missouri, Oklahoma, and Arkansas, and extends from the northeast corner of the Tier-2 sector into the Tier-3 sector of the NAME domain (Amador et al. 2004).

The areal average of precipitation in the box defines the Great Plains Precipitation (GPP) index. A similar index was used by Ting and Wang (1997) and Mo et al. (1997) to track precipitation variability in the central United States; Schubert et al. (2004) have, however, used a more meridionally extended box for index definition.⁴ Although indices remain attractive in characterizing variability because of their intrinsic simplicity,

⁴ Other index definitions: Ting and Wang's: 32.5° – 45° N, 105° – 85° W; Mo et al.'s: 34° – 46° N, 105° – 85° W; and Schubert et al.'s: 30° – 50° N, 105° – 95° W.

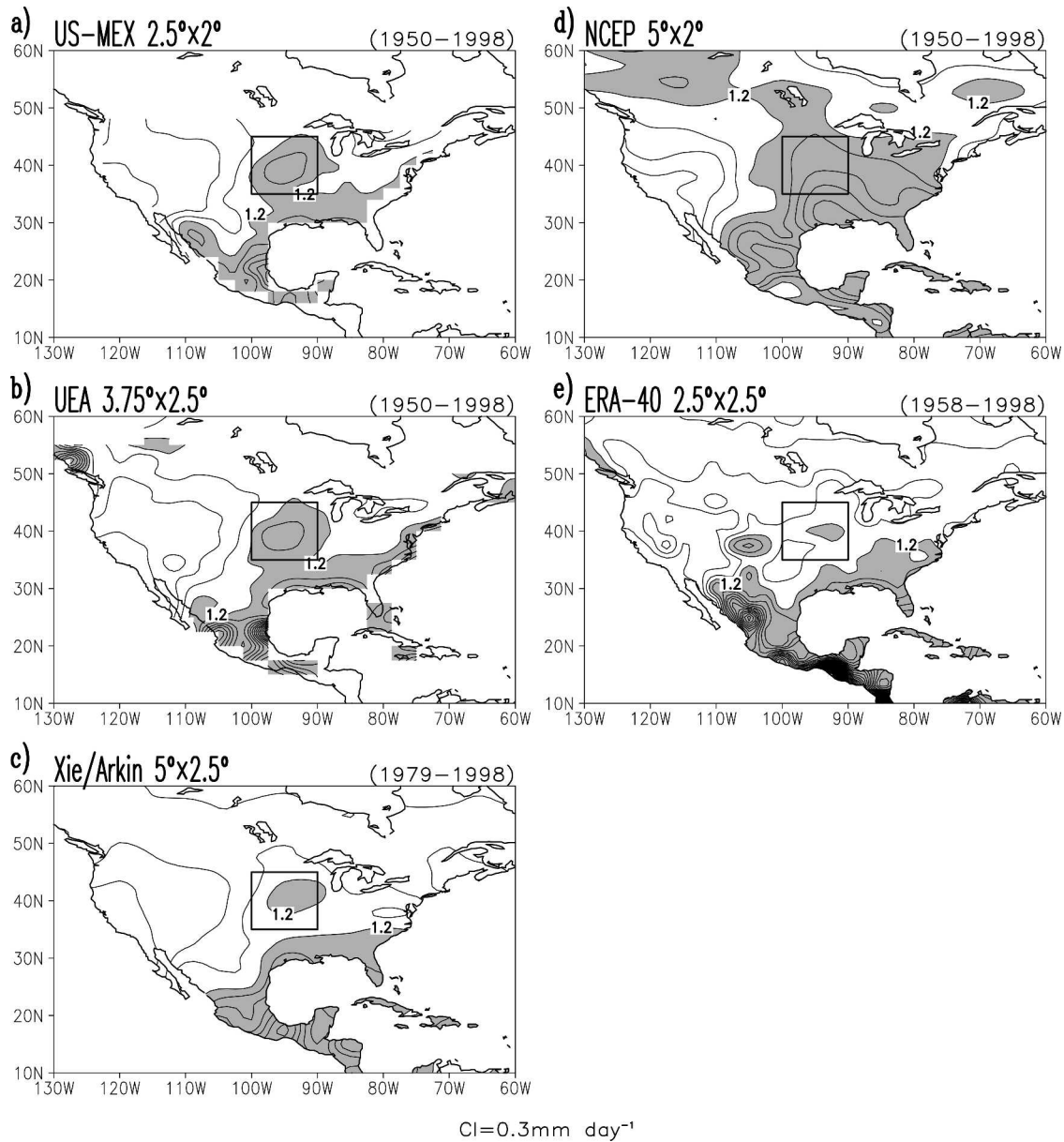


FIG. 1. Standard deviation of *monthly* precipitation anomalies during summer (Jun–Aug) in (a) U.S.–Mexico station precipitation analysis (1950–98); (b) UEA analysis (1950–98); (c) Xie–Arkin (CMAP-2, 1979–98); (d) NCEP reanalysis (1950–98); and (e) ERA-40 reanalysis (1958–98). The local maximum in std dev over the central United States in (a)–(c) helps define the Great Plains region (marked square). Areally averaged precipitation in the box defines the GPP index. Oceanic values in (c)–(e) are suppressed. Contour interval is 0.3 mm day⁻¹ and values greater than 1.2 mm day⁻¹ are shaded.

index variations cannot always be associated with a single physical mode of variability.

c. Index variations in observation and reanalysis datasets

The GPP index is shown in Fig. 3 for the warm season months. Figure 3a shows the index from the U.S.–Mexico dataset. The index exhibits both intraseasonal and lower-frequency variability: it changes sign within the summer season in 38 of the 49 analyzed summers.

The recent drought and flood events in the central United States—the early summer drought in 1988 and the 1993 summer floods—are captured in the index variations; the monthly index keeps the same sign during the entire season in these years.⁵ The GPP index

⁵ According to Fig. 3a, 1951 would be the next wettest summer, while 1976 would be the next driest summer in the Great Plains in the post-1950 record.

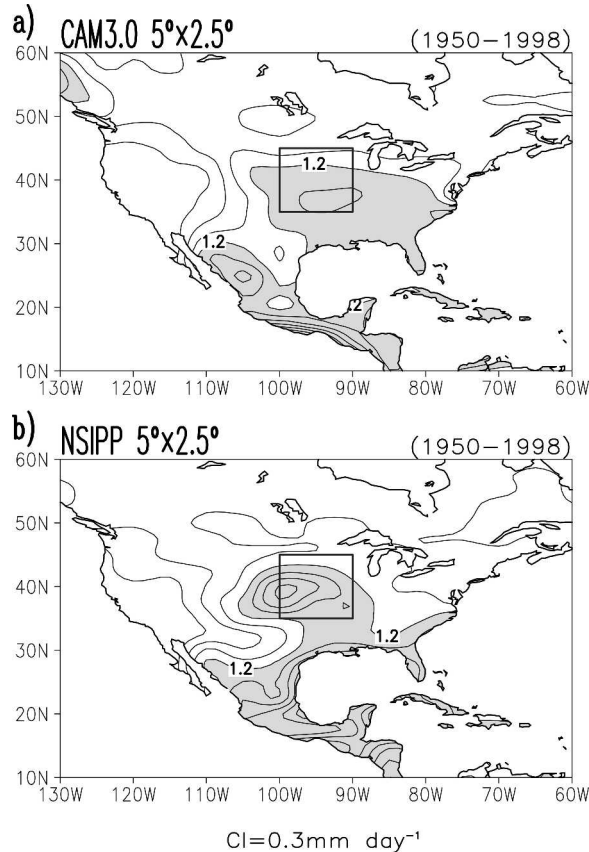


FIG. 2. Standard deviation of *monthly* precipitation anomalies during summer (Jun–Aug) in the AMIP integrations (1950–98): (a) NCAR CAM3.0 simulation (first ensemble member), and (b) the NSIPP simulation (fifth ensemble member). The marked box outlines the Great Plains region defined earlier using observed precipitation variability. Oceanic values are suppressed; contouring as in Fig. 1.

calculated using NCEP and ERA-40 reanalysis is shown in Figs. 3b,c using the same scale. Index variations are robust in the NCEP reanalysis; the JJA monthly SD being 1.21 mm day^{-1} , in comparison with 0.90 mm day^{-1} in the U.S.–Mexico dataset (Fig. 3a). The ERA-40 index, on the other hand, exhibits weaker variations, with a SD of only 0.66 mm day^{-1} . The two reanalysis indices are however closer together in tracking the anomalies (correlated at 0.77); NCEP is correlated with observations at 0.53, while ERA-40 is more strongly correlated at 0.71, all at monthly resolution.

Interannual variability is highlighted in Fig. 3 by solid, continuous lines, produced from the 1–2–1 smoothing of the summer-mean index anomalies.⁶ Figure 3a shows the smoothed indices from U.S.–Mexico (solid) and UEA (dashed) datasets, and their substan-

⁶ The smoothed index is thus based on the preceding, current, and subsequent summer means.

tial overlap attests to their closeness in the Great Plains region; the monthly summer correlation is 0.98. In contrast with observations, the smoothed reanalysis indices show an upward trend in Great Plains precipitation since the mid-1960s. Discrepancy with observations is especially pronounced in the earlier part of the record (1950–70) and leads to reduced correlations: 0.33 for NCEP and 0.55 for ERA-40, as opposed to the increased NCEP-ERA-40 correlation of 0.88. An interesting discrepancy in the latter part is the marginal representation of the 1988 early summer drought in the reanalysis datasets, particularly, NCEP.

d. Index variations in AMIP simulations

The GPP index from the AMIP simulations is shown in Fig. 4. The CAM simulation (Fig. 4a) exhibits a realistic range of variability; the JJA monthly standard deviation is 0.96 mm day^{-1} , that is, very close to the observed value. The NSIPP simulation is equally good in this respect with a 0.99 mm day^{-1} amplitude. The temporal structure of variability however leaves much to be desired in both simulations. CAM is correlated with the observed index at 0.11, while NSIPP is correlated at -0.09 , all at monthly resolution; the eight-member⁷ unsmoothed NSIPP ensemble mean (not shown) is also poorly correlated (0.04), as is the corresponding five-member CAM3.0 ensemble mean (0.15). That the 1988 and 1993 summers are not notably anomalous over the Great Plains in the model simulations is testimony to the poor temporal correlations. Precipitation is, in fact, excessive in the NSIPP simulation in the 1988 summer! The CAM and NSIPP simulations are thus unable to produce realistic *monthly* precipitation variability over the Great Plains, and the corresponding ensemble means fare no better.

But could *seasonal* (and lower frequency) variability be somewhat more realistically represented in these simulations? The question is pertinent since the models are, presently, unable to generate realistic intraseasonal variability. Smoothed versions of the indices are displayed in Figs. 4a,b to highlight the longer time scales; smoothed versions of the ensemble mean indices are also shown using a dashed line. A visual comparison of the smoothed indices with their observational counterpart (Fig. 3a) shows little traction, and this is reflected in the limited correlations: 0.25 for CAM and 0.06 for NSIPP. The ensemble means do somewhat better with 0.59 for CAM and 0.30 for NSIPP.

That still leaves open the possibility that the 1988 and

⁷ Data archiving problems during model integration precluded the use of one ensemble member.

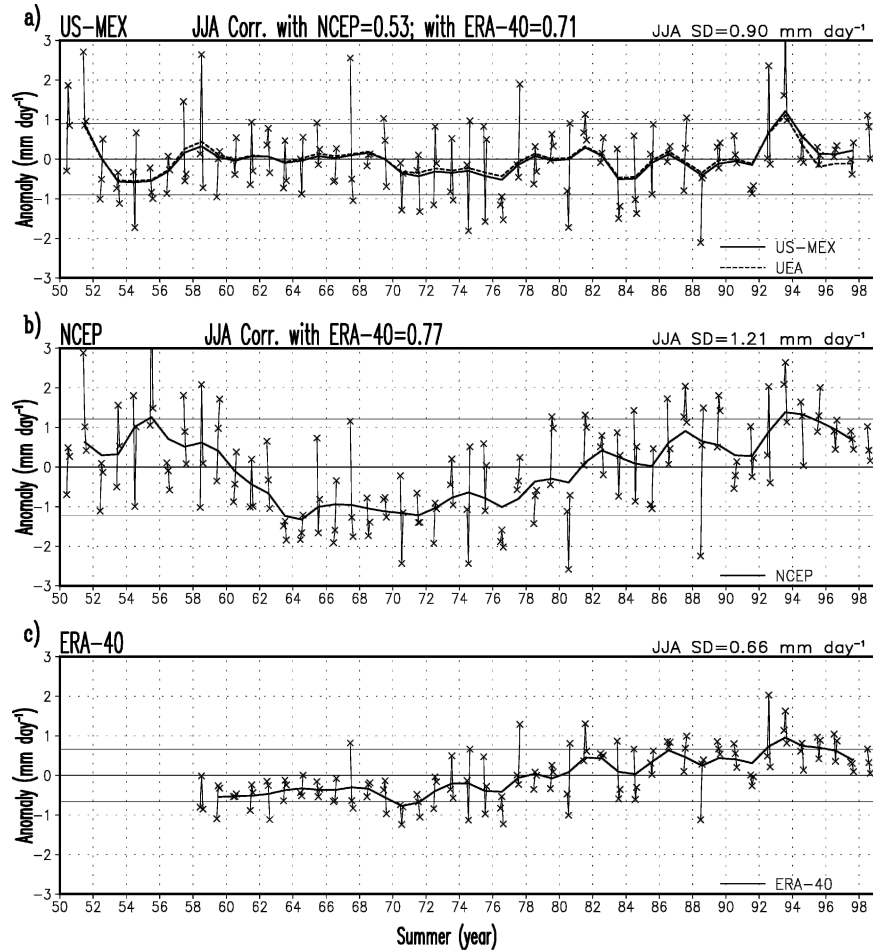


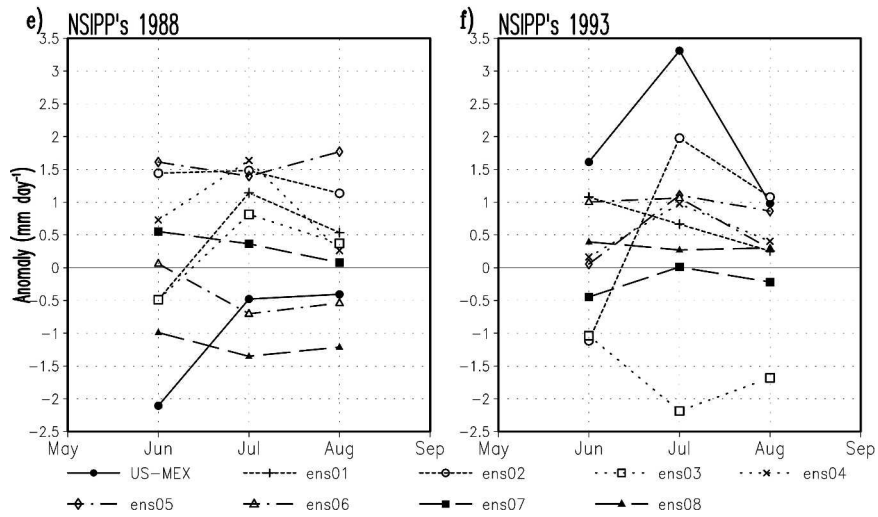
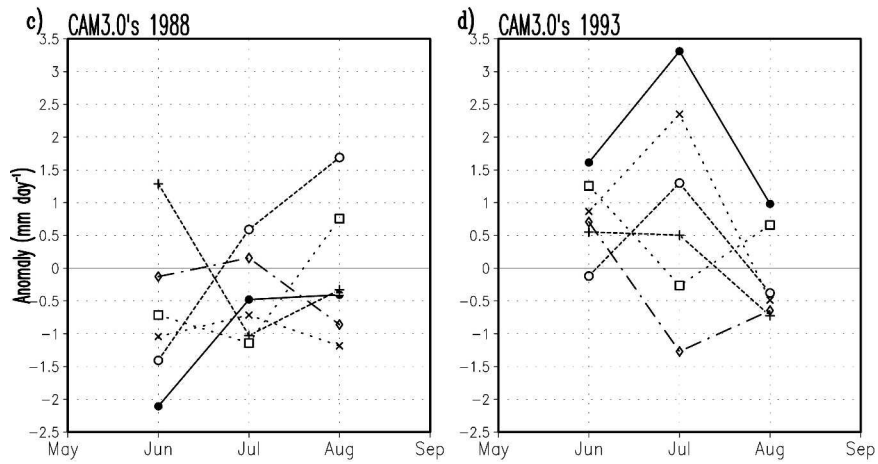
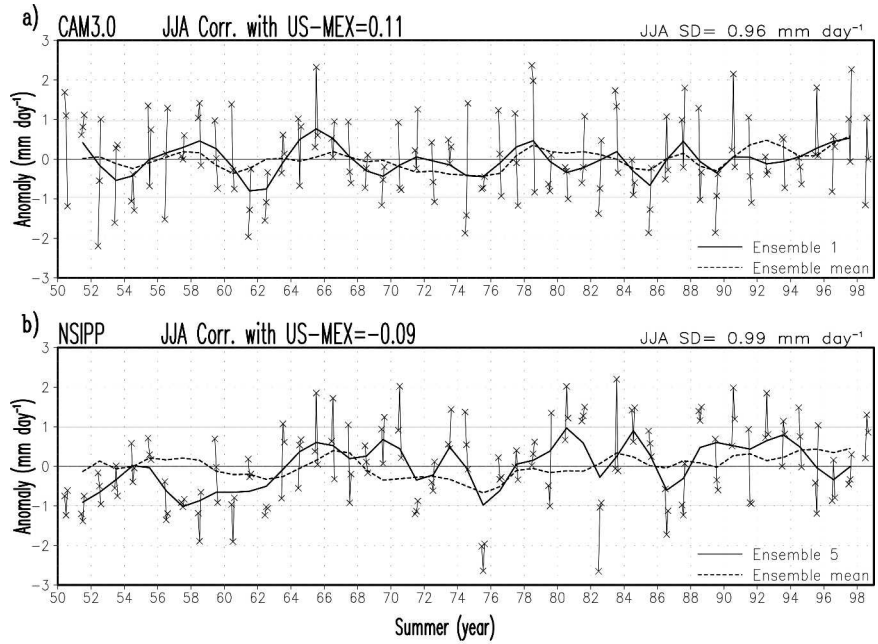
FIG. 3. GPP index anomalies in the warm season (JJA) in (a) U.S.–Mexico station precipitation analysis; (b) NCEP reanalysis, and (c) ERA-40 reanalysis. Monthly values are shown using an “x,” while the smoothed index version obtained from a 1–2–1 averaging of the seasonal mean anomalies are displayed using solid lines; horizontal lines mark the ± 1 std dev (SD) range in each panel. The dashed line in (a) shows the smoothed index from the UEA dataset for comparison. The monthly warm season SD is noted in the upper-right corner of each panel; note, the y-axis scale is the same in all panels. Monthly warm season correlations between precipitation indices in different datasets are also noted in the title line.

1993 anomalies are captured by at least some of the ensemble members in each case. The simulated precipitation anomalies are shown in Figs. 4c–f. CAM3.0 apparently starts out the warm season well, with four of the five members having the right sign. The simulation degrades thereafter, with two or more members having

the wrong sign in July and August during both 1988 and 1993. The NSIPP model, on the other hand, is clearly challenged in 1988, with six of the eight members depicting this summer as a wet season! The model compensates for this poor performance with a good show in 1993, when an equal number of the members

→

FIG. 4. Great Plains precipitation index anomalies in the warm season (JJA) in the AMIP integrations (1950–98): (a) NCAR CAM3.0 simulation (first ensemble member), and (b) NASA NSIPP simulation (fifth ensemble member). The dashed lines show the smoothed indices from the ensemble mean simulations for comparison. Otherwise, as in Fig. 3, including the y axis. Precipitation anomalies simulated by the different ensemble members for the drought and flood events of 1998 and 1993, respectively, are displayed (c), (d) for CAM3.0 and (e), (f) for NSIPP models. The continuous line with filled circles represents the observed anomaly from the U.S.–Mexico dataset, while the other lines represent the simulated anomalies by the different ensemble members of the two models: five by CAM3.0 and eight by NSIPP.



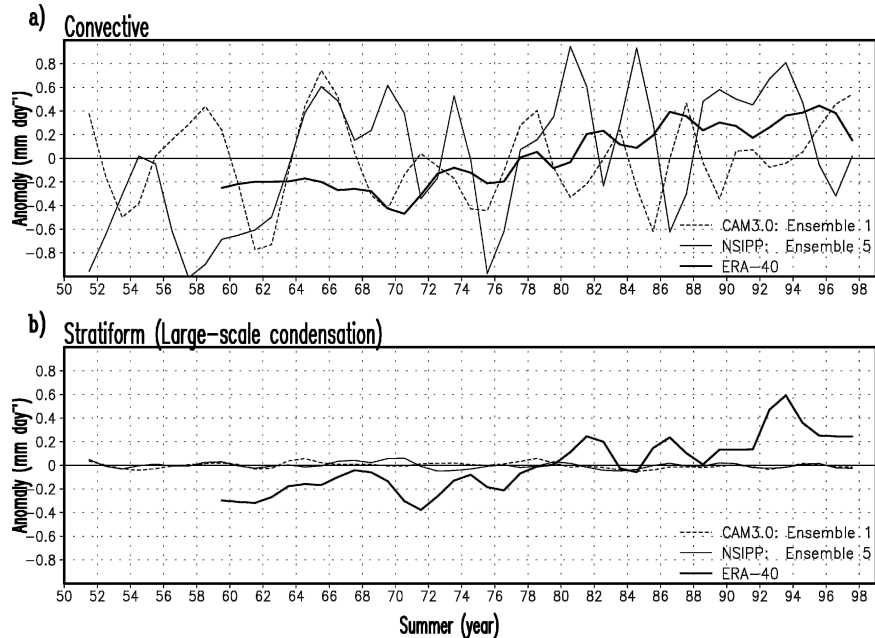


FIG. 5. Convective and stratiform contributions to the Great Plains precipitation index variations in model simulations and reanalysis during the warm season. The contributions are smoothed as described earlier. Thick solid lines denote the contribution in ERA-40 reanalysis, which begins in 1958, while the thin solid and dashed lines denote contributions in the NSIPP (fifth ensemble member) and CAM3.0 simulations, respectively. Note the small amplitude of the stratiform (large-scale condensation) component in both simulations.

get the sign (if not the amplitude) of the precipitation anomaly right. Overall, CAM3.0 appears to be more discriminating, though.

Modest values of the ensemble mean correlations should not however be taken to be reflective of the extent of SST influence on Great Plains precipitation in nature since model deficiencies could easily interfere with the realization of the potential influence. Observational analyses indicate the SST linkage to be somewhat (but not considerably) stronger. Schubert et al. (2004) report stronger links between Great Plains precipitation and Pacific SSTs in more extended NSIPP simulations, albeit at lower frequencies (time scales greater than 6 yr). Models are clearly in need of further refinements, especially in the representation of interactions between dynamical and thermodynamical processes.

e. Index variations from convective and stratiform rainfall

The convective and stratiform contributions to the smoothed GPP index in ERA-40 reanalysis and model simulations are shown in Fig. 5 using a reduced vertical scale. During summer, convection over the Great Plains can be deep (Heideman and Fritsch 1988), and the resulting convective rainfall can be comparable to the more widely produced stratiform rainfall (also called

large-scale condensation). Analysis of the surface reports of summertime precipitation frequency shows that the convective component is, in fact, quite significant over the central United States (Dai 2001). The convective and stratiform rainfall over the Great Plains is comparable in ERA-40 reanalysis (thick lines); for reasons that are unclear, both components exhibit an upward trend. The early summer drought in 1988 and the 1993 floods are both due to stratiform rain variations in the ERA-40 reanalysis: note that the convective component is positive in these periods.⁸ Distribution of the convective and stratiform rainfall is however quite lopsided in the model simulations (thin lines), with the stratiform component being almost zero! Dai and Trenberth (2004) found this to be true also in the CAM2.0 model, and attributed this to the rather early and frequent triggering of deep convection in that model. Note, the partitioning of convection also depends on the models' horizontal resolution; variations in the latter could, thus, account for some of the Fig. 5 differences.

⁸ Smoothed indices, constructed from seasonal anomalies over three summers, are unable to portray the early summer (June) drought in 1988 in Fig. 5 (and Fig. 3), but examination of the monthly, unsmoothed partitioned rainfall amounts (not shown) indicates the 1988 event to be also linked to stratiform rain variations.

4. Great Plains precipitation linkages

a. Precipitation structure

The GPP index is regressed on the U.S.–Mexico data in Fig. 6a; the index is derived from the same data, as well. Regressions are strongest over the Great Plains, as expected, but Great Plains precipitation is apparently not linked with significant precipitation anomalies elsewhere on the continent—quite unlike the case during seasonal onset of the North American monsoon, when a compensatory structure is present across the southern tier states in July (e.g., Barlow et al. 1998). The GPP index regressions on NCEP and ERA-40 reanalysis precipitation are shown in Figs. 6b,c, respectively; the indices are derived from the respective precipitation datasets. The reanalysis distributions are not as regionally confined as in Fig. 6a, but exhibit subcontinental scales, particularly NCEP's, which shows the Great Plains precipitation anomaly to be part of a much larger wet pattern covering the central and eastern United States. The ERA-40 regressions are somewhat weaker over the Great Plains ($\approx 1.2 \text{ mm day}^{-1}$), in line with expectations (cf. Figs. 1 and 3).

b. Reanalysis moisture fluxes

Moisture fluxes associated with the Great Plains precipitation anomalies are shown in Figs. 6d–g. The fluxes are obtained from 6-hourly reanalysis data, and the stationary and transient components are shown separately after vertical integration over the surface to 300-hPa layer, that is,

$$\int_{300\text{hPa}}^{P_{\text{sur}}} \bar{q} \bar{\mathbf{V}} dp/g; \int_{300\text{hPa}}^{P_{\text{sur}}} \overline{q' \mathbf{V}'} dp/g,$$

respectively. Here q is the specific humidity, \mathbf{V} the horizontal wind vector; the overbar denotes the monthly mean, and the prime the deviation from it. More precisely, stationary and transient fluxes were calculated at 0000, 0600, 1200, and 1800 UTC of each month and then averaged in order to preclude aliasing of the diurnal cycle. The NCEP surface pressure field was used in both diagnoses since this field was not readily (or freely) available in ERA-40 reanalysis; in retrospect, this choice was good for comparisons. Data from the additional lower-tropospheric level in ERA-40 reanalysis (775 hPa) was not used in computation of the vertical integral so that the two moisture fluxes can be closely compared.⁹

The stationary moisture fluxes linked with Great Plains precipitation variability in NCEP and ERA-40

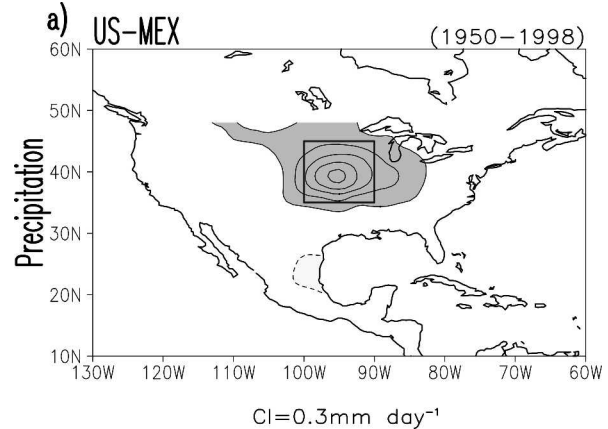


FIG. 6. Warm season regressions of the Great Plains precipitation index on (a) U.S.–Mexico station precipitation, (b) NCEP precipitation, (c) ERA-40 precipitation, (d) NCEP stationary moisture fluxes, (e) ERA-40 stationary moisture fluxes, (f) NCEP transient moisture fluxes, and (g) ERA-40 transient moisture fluxes. Note that the index and regressions are from the same monthly dataset in each case. Moisture fluxes in (d)–(g) are vertically integrated (300 hPa to the surface), and the flux convergence is also shown. Both precipitation and moisture flux convergence are contoured with the same interval (0.3 mm day^{-1}); dark (light) shading denotes areas of positive (negative) rainfall and moisture flux convergence (divergence) in excess of 0.3 mm day^{-1} magnitude; the zero contour is omitted. The vector scale for fluxes is shown at the bottom of each panel; note the 5-times larger scale in the display of the stationary panel.

reanalysis are broadly similar over North America (cf. Figs. 6d,e). In both cases, fluxes are onshore over the Gulf coast and then northeastward oriented; however, fluxes and flux convergences are stronger in ERA-40 by a factor of up to 2. Interesting differences are also evident over the American Tropics, especially, the Caribbean Sea, where ERA-40 has robust westward fluxes. The fluxes are part of a coherent, large-scale, low-level¹⁰ anticyclonic circulation that connects with the southerly fluxes over the U.S. Gulf Coast, much as in the western flank of the Bermuda high (a prominent feature of the summertime sea level pressure field over the Atlantic). It is noteworthy that flux convergence accounts for much of the Great Plains precipitation in ERA-40.

The transient moisture fluxes linked with Great Plains precipitation variability (Figs. 6f,g) are substantially smaller than the stationary ones. The vector scale in these panels is smaller by a factor of 5; the flux convergence is, however, smaller by only a factor of 2–3. The transient fluxes are westward over the eastern United States in both reanalyses, but the ERA-40 ones are stronger and more convergent, particularly, over

⁹ Separate analysis of the influence of 775-hPa data on vertically integrated moisture fluxes shows the impact to be modest.

¹⁰ Moisture weighting in the vertical integral highlights the lower-tropospheric circulation features.

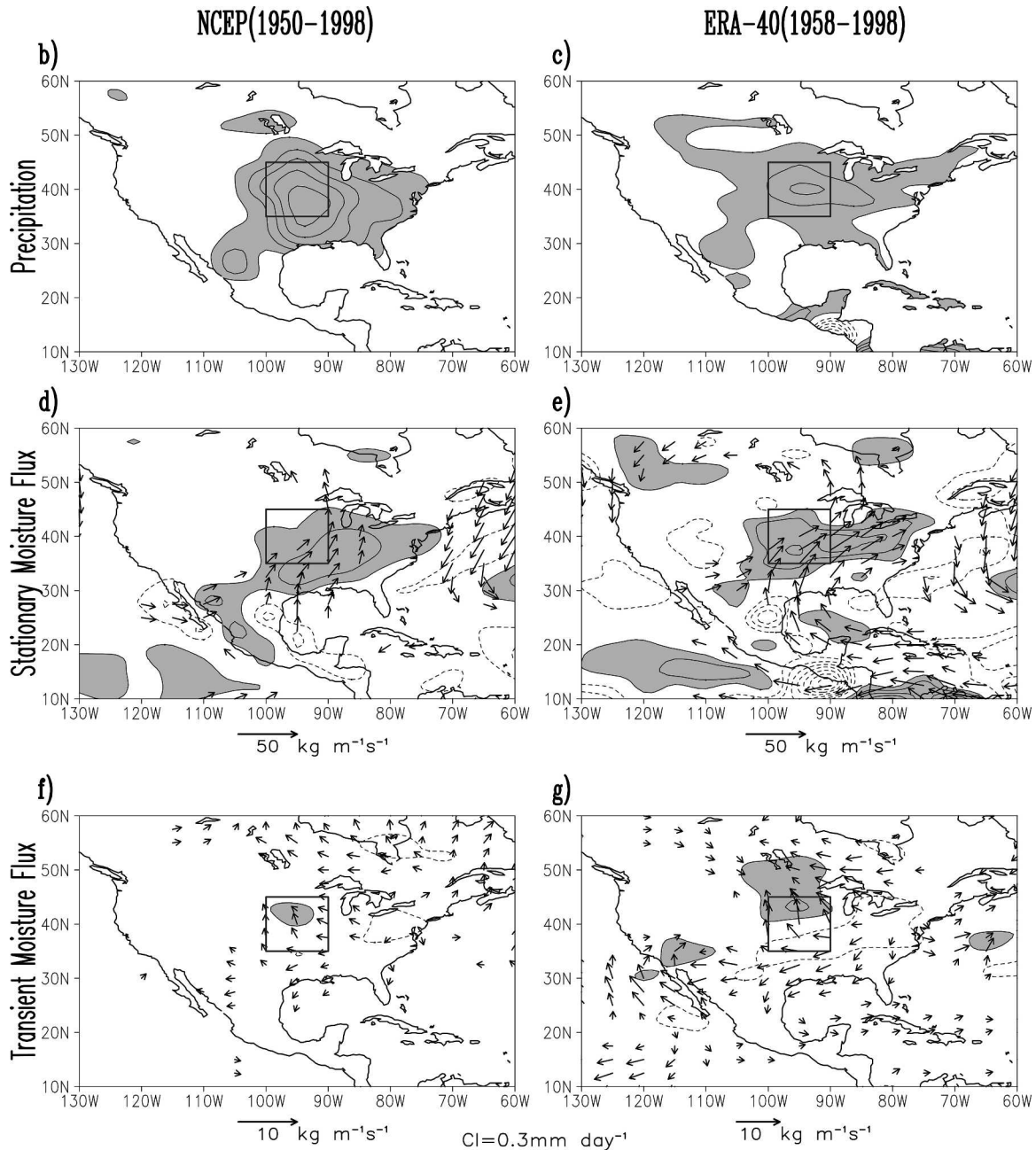


FIG. 6. (Continued)

the northern Great Plains, where their precipitation contribution is significant. The transient fluxes are related to synoptic storm activity over the eastern United States, which is not as strong as in winter but still consequential for moisture flux convergence.

In summary, anomalies in monthly averaged Great Plains precipitation are associated with significant stationary moisture fluxes. Convergence of these fluxes accounts for a large fraction of the precipitation anomaly over the Great Plains in ERA-40, but not in

NCEP, implying a rather different atmospheric water balance over this region, at least in summer.

c. Simulated precipitation and moisture flux variability

Precipitation and moisture flux anomalies accompanying GPP index variations in the model simulations are displayed in Fig. 7. Both models generate coherent precipitation anomalies over the Great Plains, that are closer to observation (Fig. 6a) than reanalyses; the NSIPP one is slightly stronger. The moisture fluxes and

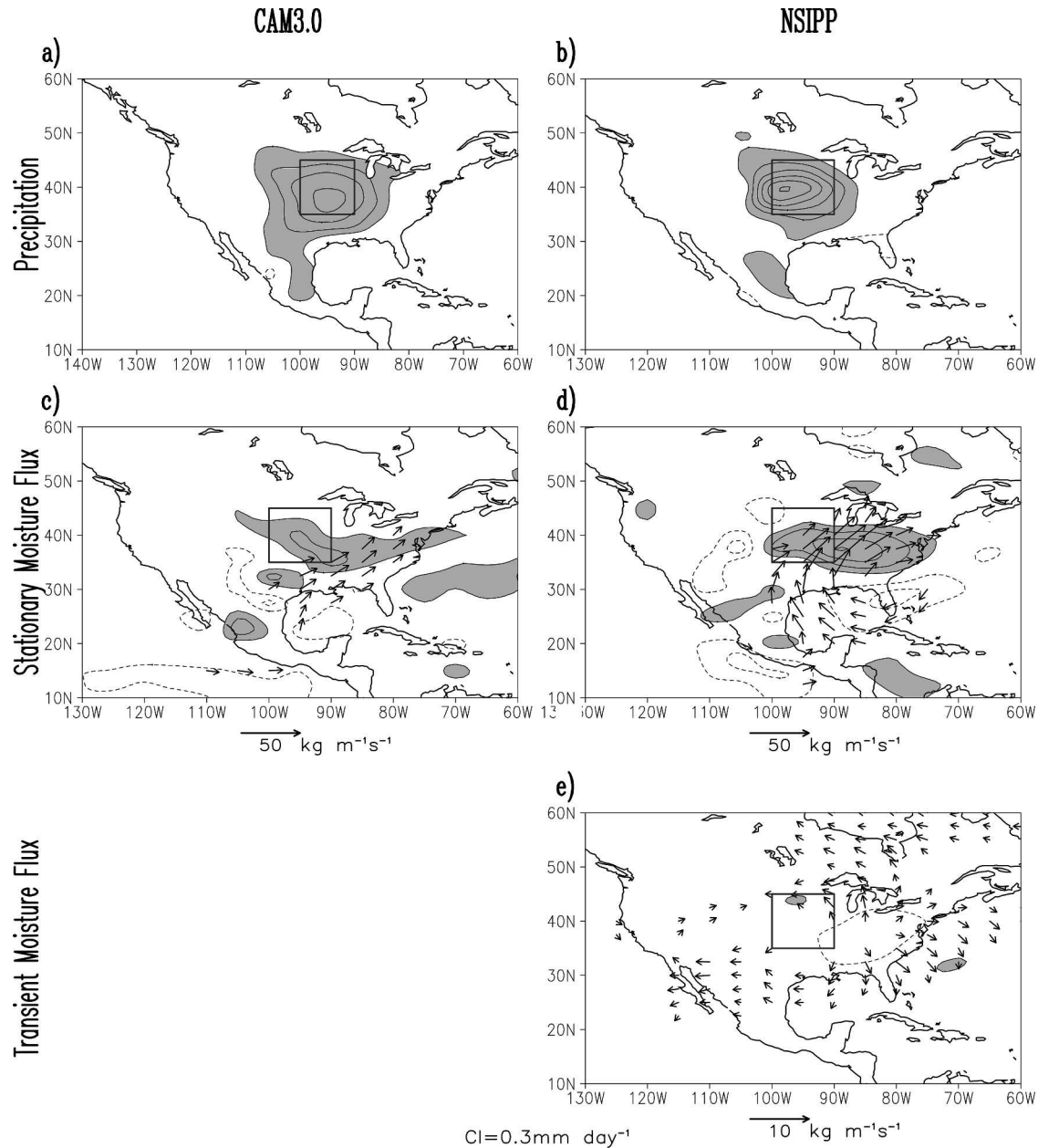


FIG. 7. Warm season regressions of the Great Plains precipitation index in AMIP simulations (1950–98): (a) CAM3.0 precipitation, (b) NSIPP precipitation, (c) CAM3.0 stationary moisture fluxes, (d) NSIPP stationary moisture fluxes, and (e) NSIPP transient moisture fluxes. Note that the index and regressions come from the same monthly dataset in each case. All NSIPP regressions are from the fifth ensemble member while the CAM ones are from the first ensemble member. Transient fluxes are not shown for CAM3.0 since the zonal component was not archived; otherwise, as in Fig. 6.

their convergence are shown in Figs. 7c–e. The focus is on the stationary component since it is dominant and also because the transient component could not be calculated for the CAM simulation as this field was unavailable in the online data archives at NCAR. The moisture fluxes are quite different in the two simulations. The CAM fluxes suggest that GPP variations are

accompanied by a low-level circulation over the southeastern United States, with a limited transport over the Gulf of Mexico in contrast with the coherent anticyclonic structure with an extended fetch that is present in the NSIPP simulation (and ERA-40 reanalysis). Not surprisingly, CAM is unable to generate sufficient moisture flux convergence over the Great Plains. The

NSIPP simulation, on the other hand, has quasi-realistic moisture fluxes, especially, in comparison with the ERA-40 fluxes.

d. Diagnosed and simulated evaporation

The relative contribution of local and remote water sources in generation of Great Plains precipitation variability motivates the examination of the evaporation field. Evaporation observations are, unfortunately, rather limited and seldom representative of the larger-scale hydroclimate conditions. Good long-term measurements are generally available only in sublatitude-longitude degree basins [e.g., the United States Department of Agriculture (USDA) monitored watersheds, Oklahoma Mesonet] and, as such, the large-scale evaporation field must often be diagnosed from reasonably validated land surface models driven by circulation, temperature, and precipitation observations. Note, the reanalysis evaporation is constrained only by circulation and temperature observations, that is, less directly.

Two evaporation diagnoses are analyzed here: The first is produced at NOAA CPC from a one-layer hydrological model (Huang et al. 1996; more information available online at <http://www.cpc.ncep.noaa.gov/soilmst/index.htm>). The model is driven by observed surface air temperature and precipitation and yields evaporation and runoff estimates for the 344 climate divisions: the model is tuned with observed runoff data in Oklahoma and estimates are available for the 1931–present period. The second diagnosis was conducted at COLA using their Simplified Simple Biosphere model (SSiB) (Xue et al. 1991). The diagnosis was undertaken for the 1979–99 period and is referred as the Global Offline Land surface Data-set (GOLD, more information available online at <http://www.iges.org/gold>; Dirmeyer and Tan 2001).¹¹

The GPP index regressions on diagnosed evaporation are shown in Figs. 8a,b. The GOLD estimates are almost a factor of 3 larger than the CPC ones, and this discrepancy cannot be attributed to the record-length differences. Interestingly, both estimates depict a maximum in the southwest corner of the boxed region (i.e., Oklahoma), which supplies the runoff observations for model tuning, at least in CPC's diagnosis. The corresponding regressions on the NCEP and ERA-40 reanalysis evaporation fields are shown in Figs. 8c,d, respectively: note that reanalysis evaporation is not con-

strained by precipitation and runoff observations. The reanalysis evaporation anomalies over the Great Plains are, apparently, as far apart as the two diagnosed anomalies; the NCEP anomaly ranges from 0.1 to 0.3 mm day⁻¹—not unlike the GOLD estimates—while the ERA-40 anomaly is not even up to the contouring threshold (0.1 mm day⁻¹), much like the CPC-based estimate.

The evaporation anomalies accompanying Great Plains precipitation variations in the model simulations are shown in Figs. 8e,f. They are phenomenally strong, reaching 1.0–1.2 mm day⁻¹; in both cases, the anomalies are focused over the Great Plains. The very large values of local evaporation in the models—up to 4 times larger than the highest observationally constrained estimate (i.e., NCEP's)—suggest a significantly different view of the anomalous atmospheric water balance, one in which local water sources (precipitation recycling) contribute overwhelmingly to Great Plains precipitation variability. For example, evaporation contributes nearly twice as much as the stationary moisture fluxes to Great Plains precipitation variability in both CAM and NSIPP simulations. The case is quite the opposite in the reanalyses, with the stationary moisture flux contributions being dominant; the flux convergence is about 1.5 times larger than evaporation in NCEP and even larger in ERA-40 data. [The finding of the dominance of evaporation over moisture flux convergence in the NSIPP model explains why Koster et al. (2003) find land–atmosphere feedback to be so important in accounting for the July precipitation variance in NSIPP simulations of Great Plains hydroclimate variability.]

Intercomparison of both evaporation anomalies and their relative contribution in generating Great Plains precipitation variability suggests that these anomalies are, perhaps, too strong in the model simulations—possibly outliers in comparison with the reanalysis and diagnosed evaporation estimates. Although this assessment will need to be corroborated from multimodel estimates of evaporation that will be produced by the Global Soil Wetness Project (GSWP-2, version 2; Dirmeyer et al. 2002; more information available online at <http://grads.iges.org/gswp2/>), it appears that land surface–atmosphere interactions are overemphasized in the models, at least in context of the warm season hydroclimate variability over North America—a distinct possibility if the model land surface schemes were tuned using climatological reanalyses data alone. The model evaporation climatologies over the United States (especially NSIPP's) are comparable to the reanalysis counterparts, but are

¹¹ The precipitation used in generating the GOLD dataset is highly correlated with the U.S.–Mexico precipitation data; the GPP indices are correlated at 0.96.

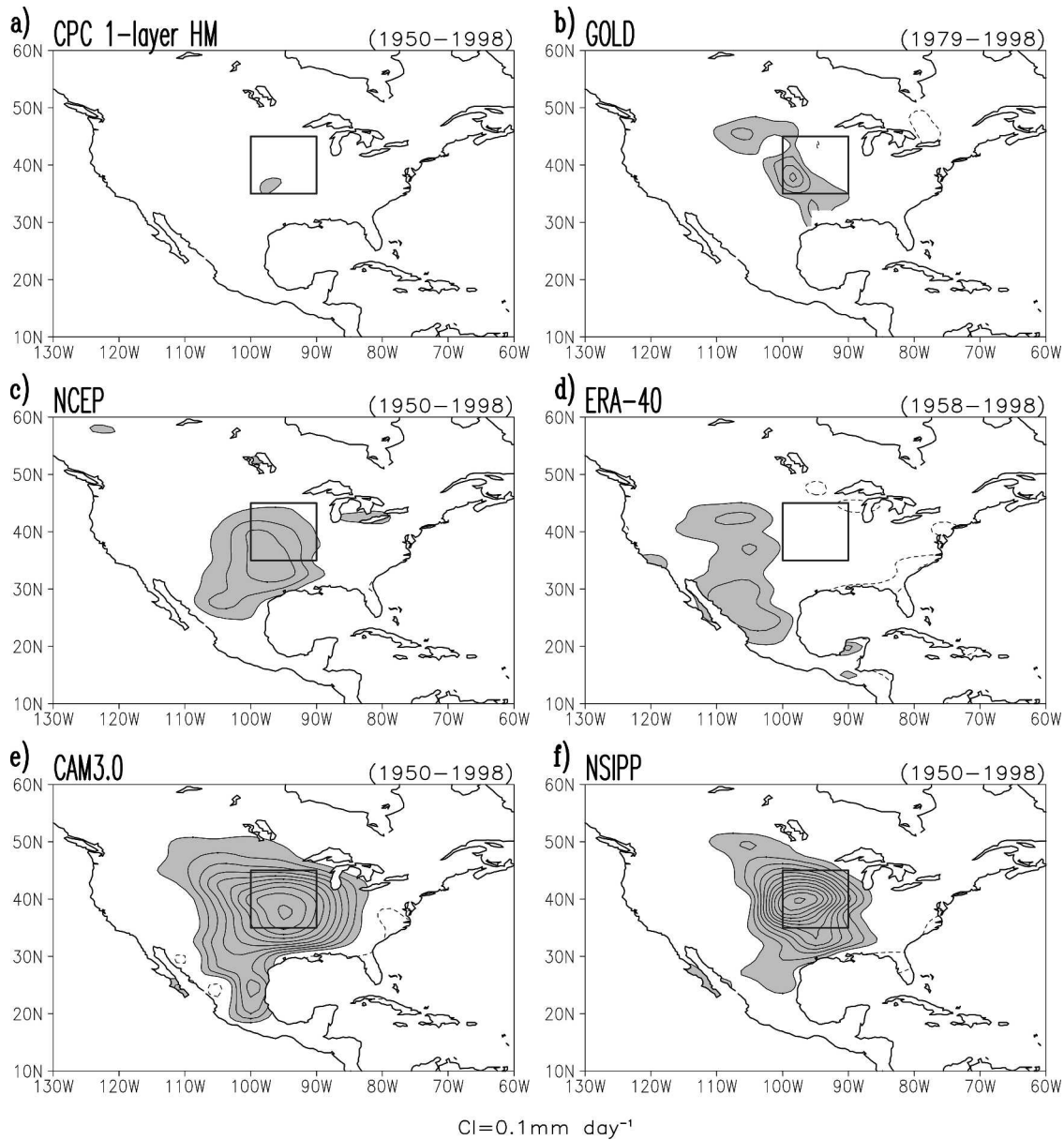


FIG. 8. Warm season regressions of the Great Plains precipitation index on evaporation (surface latent heat flux): (a) evaporation diagnosed from NOAA/CPC one-layer hydrologic model (see text for details), (b) another diagnosis of evaporation (GOLD dataset; see text for details), (c) NCEP evaporation, (d) ERA-40 evaporation, (e) CAM3.0 evaporation (first ensemble member), and (f) NSIPP evaporation (fifth ensemble member). Note that the regression period stated in the title line varies somewhat. Regressions in (a) are against the GPP index constructed from the U.S.–Mexico dataset; in the remaining panels, the index and regressions are from the same dataset. The contour interval and shading threshold is 0.1 mm day^{-1} , with positive values shaded dark; the zero contour is omitted in all panels.

much too strong vis-a-vis the diagnosed GOLD and CPC evaporation climatologies—by up to a factor of 2.

e. Observed and simulated SST links

The SST links to Great Plains precipitation variability are identified from correlations of the smoothed

GPP indices (shown in Figs. 3–4) and displayed in Fig. 9. The smoothed index versions are used in order to highlight linkages on the seasonal to interannual time scales, while correlations are computed instead of regressions in order to assess the significance of SST linkages in the context of interannual variability. Correla-

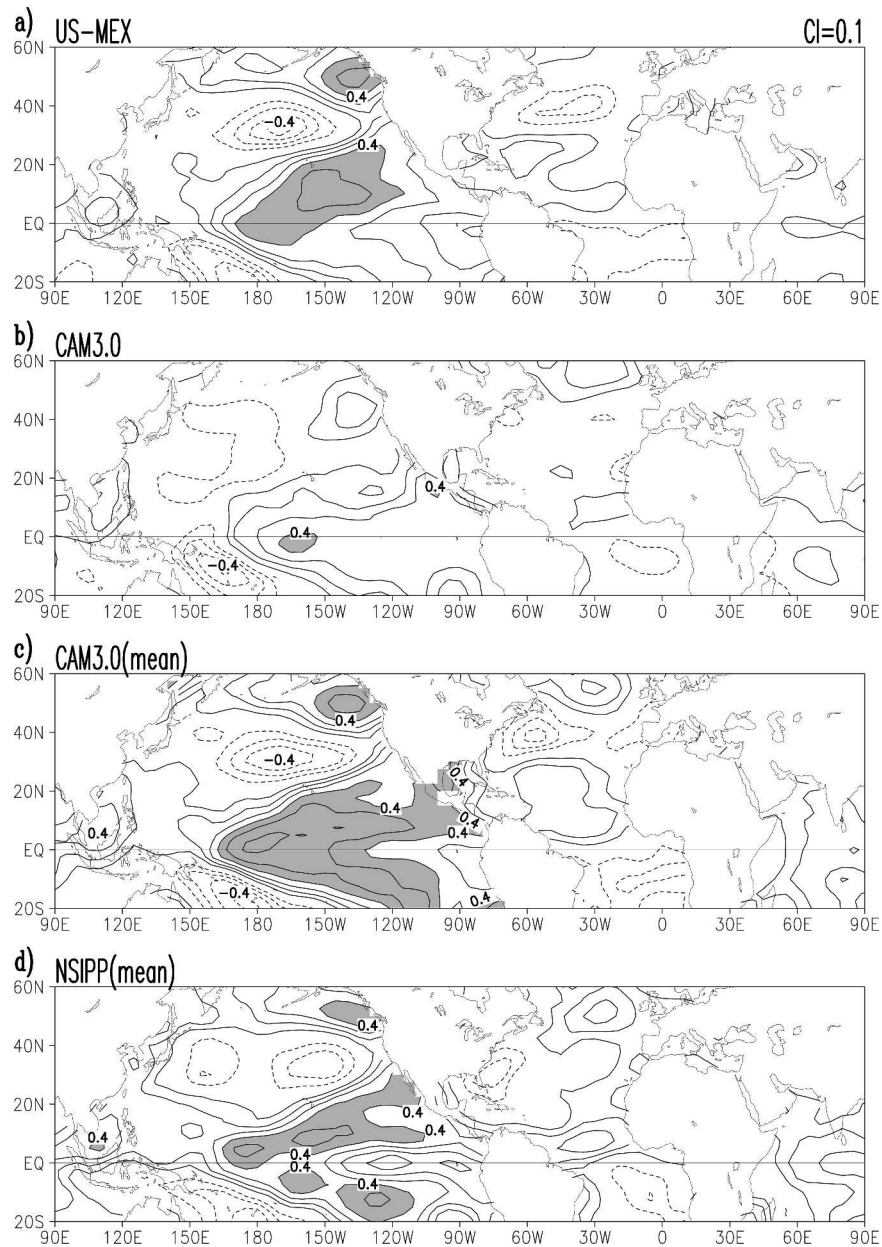


FIG. 9. Warm season SST correlations of the smoothed Great Plains precipitation index (1950–98). The smoothed index is from (a) the U.S.–Mexico station precipitation analysis, (b) CAM3.0 simulation (first ensemble member), (c) CAM3.0’s five-member ensemble mean simulation, and from (d) NSIPP’s eight-member ensemble mean simulation. Correlations have been smoothed using adjacent grid points (smth9 in GrADS). Contour interval is 0.1 and dark (light) shading denotes positive (negative) correlations in excess of 0.4 magnitude. The zero contour is omitted in all panels.

tions of the precipitation index derived from the U.S.–Mexico station data are shown first in Fig. 9a, as they are the simulation target. SST correlations exhibit a coherent, basin-scale structure that resembles the Pacific decadal variability pattern in many respects. The largest correlations (~ 0.5) are in the Gulf of Alaska,

the midlatitude Pacific (date line sector),¹² and in a northeastward-oriented band emanating from the

¹² This region exhibits the strongest correlation (~ 0.5) with the unsmoothed version of the seasonal GPP index.

equatorial central Pacific. The correlation structure rules out contemporaneous linkage between ENSO and the smoothed, seasonally averaged Great Plains precipitation.¹³ The finding on connections with the extratropical Pacific SSTs is not a new one; Ting and Wang (1997), Higgins et al. (1999), Nigam et al. (1999), Lau and Weng (2000), and Barlow et al. (2001) have all investigated aspects of this linkage.

SST correlations of CAM's smoothed GPP indices are shown in Figs. 9b,c. Correlations of the first ensemble member's index exhibit coherent structure in the tropical Pacific, similar to the target structure (Fig. 9a). Correlations of the ensemble mean index are even closer to Fig. 9a; note the striking similarity in the mid-latitude basins. The correlations are however somewhat stronger in the central equatorial Pacific (~ 0.6), pointing to this region's greater connectivity with the Great Plains in CAM3.0. The corresponding correlations of NSIPP's ensemble mean index (Fig. 9d) are qualitatively similar, but are not as close to the target structure as CAM's; especially in the western midlatitude basins. Longer AMIP simulations with the NSIPP model (Schubert et al. 2004) indicate stronger links with Pacific SSTs in the entire tropical basin (correlations ~ 0.6 – 0.7 using an all-year index); reasons for the discrepancy are unclear, but the use of highly smoothed SSTs and GPP index (retaining 6-yr or longer time scales) likely contributes to the higher correlation.

The extent to which Figs. 9b,c differ is surprising because the internally generated (random) variability should have been filtered out during computation of the correlation. As discussed earlier (cf. footnote 3), an ensemble of AMIP-type climate simulations can help in apportioning a *particular* summer's anomaly into its internal and SST-forced variability components. But a simulation ensemble would be deemed to have considerable redundancy in the context of extraction of the *characteristic* (dominant) patterns of interannual variability, especially, if each simulation was of sufficient duration [e.g., the case here (~ 50 yr)]. Correlation analysis on a single ensemble member of such length should have sufficed in filtering the internally generated (random) component of variability.

¹³ This is consistent with Barlow et al.'s (2001) analysis, which shows a *monthly* evolution in ENSO's impact on U.S. precipitation (cf. Fig. 5); the impact is, in fact, opposite at the beginning (June) and end (August) of the warm season, particularly along the East Coast and in the Great Plains. Absence of the ENSO signature in SST links of the *seasonally* averaged GPP index is thus not surprising; the 1–2–1 smoothing of the GPP index across three summer seasons must further diminish the linkage.

f. Antecedent SST links in observations

The SST links shown above are all contemporaneous and, hence, not revealing of the direction of influence. Causality is investigated by computing correlations of the July GPP index (derived from the U.S.–Mexico station data) with antecedent SSTs. July's index is chosen as a reference since the standard deviation of monthly precipitation is strongest in this month and, also, because July is in the middle of the warm season. The SST-leading correlations are shown in Fig. 10 at monthly resolution starting in April; the correlations are computed with the unsmoothed version of the index. The antecedent correlations are seldom larger than 0.4 but exhibit a coherent structure similar to that seen earlier (Fig. 9a).

The antecedent SST structure over the Pacific (Figs. 10a–c) is broadly similar to the contemporaneous SST links (Fig. 10d), especially at basin scales except for regional developments in the extratropical basin (atmosphere forced?). A meridional expansion of the equatorial Pacific feature with time is also evident. The shape evolution is intriguing, with the focal point moving to the northern off-equatorial latitudes in summer. But, are the 0.3–0.4 correlations significant, especially against the backdrop of decadal variability in the Pacific and Atlantic basins? A careful examination of this issue is beyond the scope of this paper, but a rudimentary analysis involving SST correlations with a randomized version of the GPP index yields contemporaneous correlations in the ~ 0.2 range in July, that is, marginally weaker than those in Fig. 10d. The obtained correlation structure (not shown) is however quite different (incoherent) from that in Fig. 10d, particularly in the eastern Pacific.

Correlations with the randomized index are however not devoid of coherency in the Atlantic basin. For this reason, the interesting evolution of Atlantic SSTs in Fig. 10 is noted, but not further discussed. Three zonally oriented bands characterize the precursor-period structure, especially, in May–June. The banded SSTs are, in fact, reminiscent of the interhemispheric variability mode (cf. Fig. 10 in Ruiz-Barradas et al. 2000), which is also energetic in spring.¹⁴ Interestingly, the bands in the extratropical Atlantic flip sign in July but the significance of this, if any, is unclear. Additional lag–lead analysis and modeling experiments are clearly needed to understand the SST linkages and their significance for U.S. hydroclimate variability.

¹⁴ The mode has also been referred to as the Pan–Atlantic decadal oscillation pattern (Xie and Tanimoto 1998).

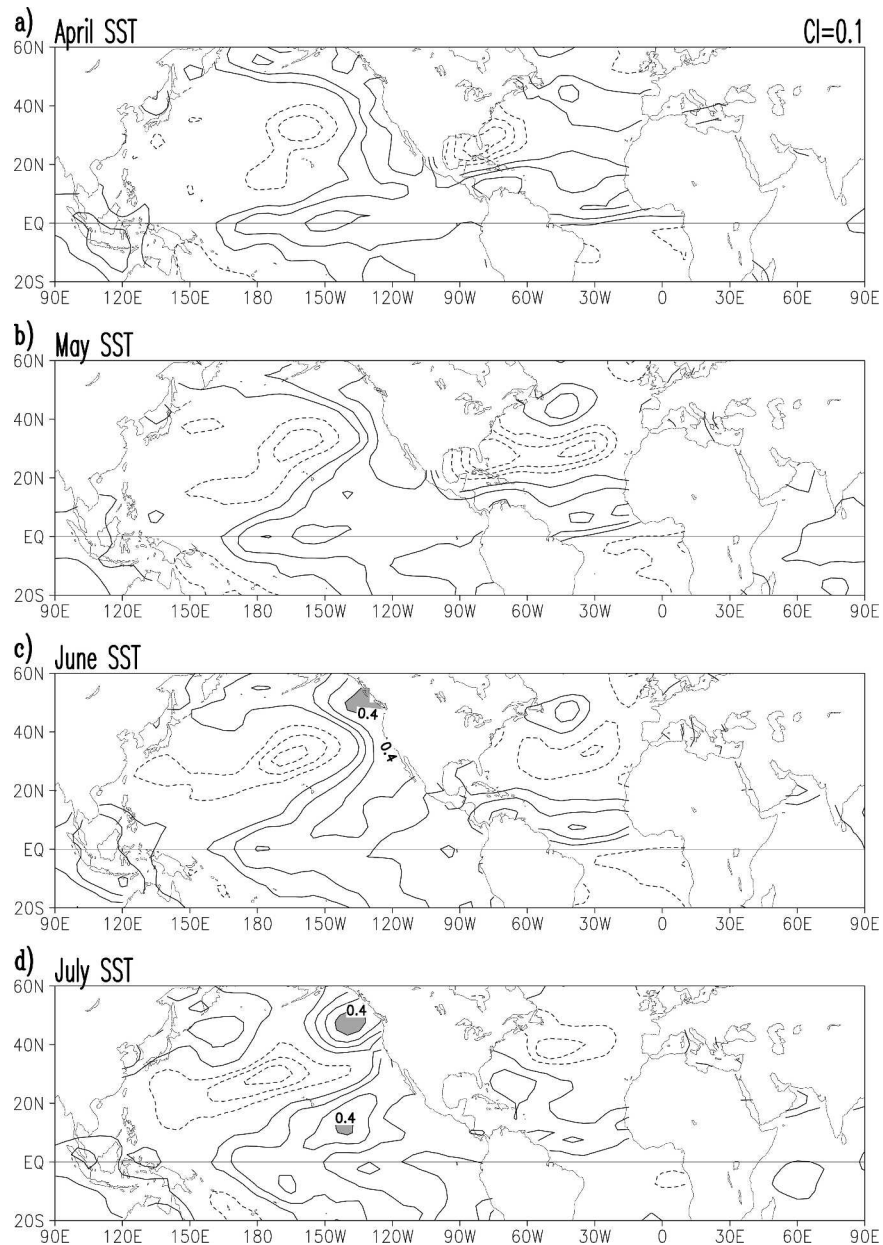


FIG. 10. SST-leading correlations with the Jul Great Plains precipitation index (1950–98). The index is derived from the U.S.–Mexico station precipitation dataset, and correlations are computed with the unsmoothed version of the index: (a) Apr SST correlations, (b) May SST correlations, (c) Jun SST correlations, and (d) Jul SST correlations (contemporaneous). Correlations have been smoothed using adjacent grid points (smth9 in GrADS). Contour interval is 0.1 and dark (light) shading denotes positive (negative) correlations in excess of 0.4 magnitude. The zero contour is omitted in all panels.

5. Recurrent patterns of warm season SST and geopotential (Φ_{700}) variability

The analysis moves away from its continental-centric precipitation focus in this section. The Great Plains precipitation index is no longer the fulcrum, but the target

here. The motivation stems from generic concerns associated with physical indices, namely, that index variations can reflect the superposed effects of two or more independent modes of variability, thereby confounding understanding of the variability mechanisms. There is already some indication of the GPP index's linkage

with the Pacific and Atlantic basins that display rather different spatiotemporal variability. Unraveling the contribution of the different variability modes in GPP index variations should advance the understanding, modeling, and prediction of Great Plains hydroclimate variability.

The SST and lower-tropospheric geopotential (Φ_{700}) variability during boreal summer months (JJA) is objectively analyzed here. Geopotential height compactly represents the winds in the extratropical domain (the region of interest), and its variability at the 700-hPa level is analyzed in order to focus on the circulation component that is important for moisture transports.¹⁵ Having a variable each from the ocean and atmosphere precludes the analysis from being SST centric (as in Barlow et al. 2001) or Great Plains centric (as in the preceding sections).

The analysis strategy is influenced by Lanzante's (1984) study, published two decades ago. The study is notable for several reasons: it provided the first objective analysis of interannual circulation variability in the warm season months; it assessed the circulation's linkage with Pacific and Atlantic SSTs within the framework of a single analysis; it corroborated important aspects of Namias's (1983; and earlier papers) analysis of antecedent/coincident drought circulations and SSTs, in particular, by showing the presence of a Pacific–North American (PNA)-like circulation pattern in the spring and summer months (i.e., well outside of the winter season); and it extended the correlation analysis technique (Prohaska 1976) through the use of varimax rotation.

The present analysis is motivated by the need to corroborate Lanzante's (1984) findings using a longer observational record—one that includes data from both before and after the 1976–77 climate transition (e.g., Trenberth 1990). Lanzante analyzed the 1949–78 period (i.e., essentially, the pretransition period). Rotated principal component analysis (RPCA) is used to identify the recurrent patterns here, as opposed to rotated canonical correlation analysis in Lanzante. The RPCA method analyzes the structure of cross-correlation and autocorrelation matrices whereas the canonical correlation technique focuses only on the former. Despite this difference, the two methods yield similar results, as ascertained from the RPCA of the 1949–78 record. The leading structures are similar to those shown in Lanzante; minor pattern differences can be as easily attributed to SST and geopotential data differences as to the analysis method differences.

¹⁵ The 850-hPa level was not chosen because of its being below the surface over large areas of North America, and because it was deemed to be somewhat disconnected from the upper-level flow (i.e., the medium connecting remote regions).

The combined variability of SST (Hadley) and 700-hPa geopotential (NCEP reanalysis) in the extratropical Pacific and Atlantic sectors (25°–75°N, 155°E–15°W) during the 1950–98 warm season months of June–August is analyzed. The variables are scaled by $(\cos \theta)^{1/2}$ to achieve grid-area parity on a regular latitude–longitude grid, and put on par with each other by normalizing their anomalies by the square root of their spatially integrated temporal variance; the advantages of such a normalization are discussed in Nigam and Shen (1993). Nine loading vectors are rotated and the resulting two that are related to Great Plains hydroclimate variability are discussed in this section. These modes are robust in that they are also obtained from rotation of the six leading loading vectors.¹⁶

a. *The Pacific connection*

The rotated principal component (PC) most strongly correlated with the GPP index in the warm season months is shown in Fig. 11d. The correlation is -0.43 ; it is the seventh leading mode in a ranking based on accounting of the SST and Φ_{700} variance in the analysis domain. The SST anomalies are prominent in the Gulf of Alaska and in the central and eastern equatorial Pacific; the causative influence of the latter is being investigated. The covariant Φ_{700} anomalies are confined to the PNA sector with a structure that is somewhat reminiscent of the wintertime PNA pattern (e.g., Wallace and Gutzler 1981; Nigam 2003). The negative SST anomalies in the Gulf of Alaska likely arise from enhanced westerlies and, consequently, enhanced surface fluxes and Ekman pumping in that sector, assuming that 700-hPa anomalies are representative of the near-surface circulation as well, a likely scenario. The SST and geopotential anomalies resemble a leading summer pattern in Lanzante's analysis (1984; Fig. 2c) except for the missing trough over the southern states in Fig. 11a. The PNA-like, warm season height anomalies are referred to as the “Great Plains” pattern in Lanzante since they are structurally similar (but oppositely signed) to the composited anomalies for the 1952–54 drought summers (Fig. 4 of Namias 1983).

The PC exhibits both intraseasonal (defined by a sign change within a season) and lower-frequency variability; the sign changes in 27 of the 49 summer seasons. The PC is positive during the 1988 summer (a recent short drought) and in other summers as well (e.g., 1970, 1973, 1984), some of which were drier than normal (cf.

¹⁶ Analysis of an extended warm season, with an additional month at the beginning (May) or the end (September), yields the same modes, as does the analysis in a larger domain (20°S–75°N, 0°–360°).

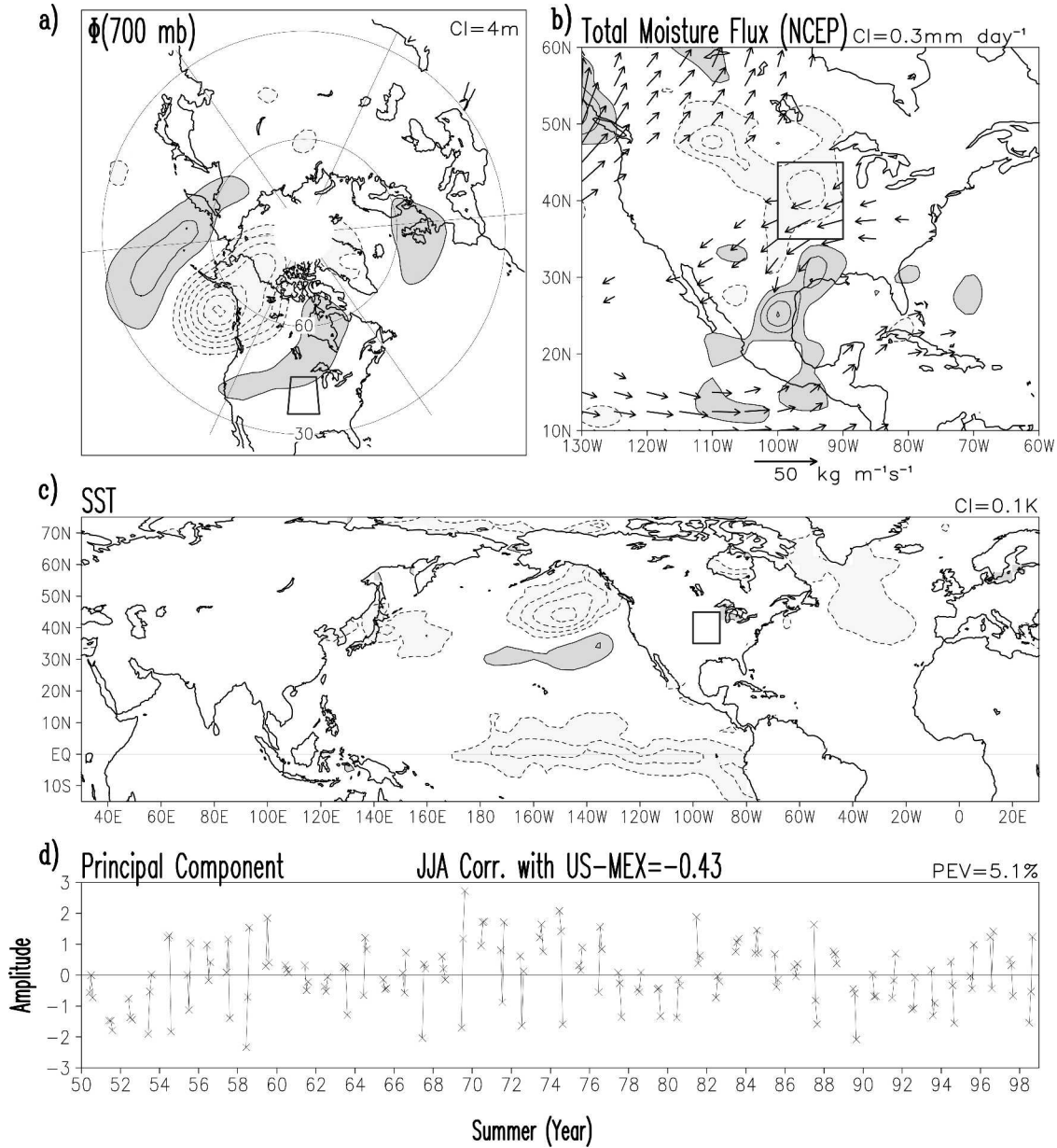


FIG. 11. The Pacific connection (PNA) variability in summer. (d) The rotated PC that correlates most strongly with the Great Plains precipitation index (U.S.–Mexico station database); the correlation is -0.43 . An RPCA of combined SST and Φ_{700} variability during the 1950–98 summers is conducted; this is the seventh PC in a ranking based on explained variance (5.1%). (a) The geopotential loadings and (c) the SST loadings. (b) PC regressions on the total (stationary + transient) NCEP moisture flux and its convergence. Contour interval and shading threshold is 4 m for the geopotential, 0.3 mm day⁻¹ for moisture flux convergence, and 0.1 K for SST.

Fig. 3a). Given the role of the 1952–54 drought in the naming of this anomaly pattern, it would be of some interest to examine the drought's representation in Fig. 11d; unfortunately, the drought is not captured since negative PC values indicate wetness (Fig. 11b). According to the PC, the 1950–53 summers is a wet period, whereas in nature (Fig. 3a) the drought onset occurred in 1952. The reasons for this discrepancy are not clear

but, then, not all dry periods are represented by this mode of variability, especially since it explains only a modest fraction ($\sim 18\%$) of the precipitation variance over the Great Plains. On the other hand, can the undertaken RPCA be tainted by the considerable departure of NCEP reanalysis from observed hydroclimate variations (cf. Figs. 3a,b; NCEP produces a wet period in the 1950s!)? Perhaps not since the reanalysis proce-

ture generally results in rather limited modification of the rotational circulation (Φ_{700}). Unfortunately, the ERA-40 reanalysis begins in 1958, precluding a comparative analysis of the 1950s drought circulation.

The vertically integrated moisture fluxes (stationary + transient) associated with this mode of variability are shown over North America in the Fig. 11a. Both the flux and its convergence (shaded) are dominated by the stationary component. The fluxes are southwestward oriented and divergent over the central United States, including the Great Plains, leading to this PC's negative correlation with the GPP index. The southwestward orientation is, of course, a result of the anomalous circulation structure, in particular, the southwest-to-northeast tilt of the ridge over the northern-tier states. The flux vectors diverge as they encounter the Rocky orography, with the southward branch opposing the climatological low-level jet, which transports phenomenal amounts of moisture northward. Not surprisingly, fluxes are divergent to the north and convergent to the south.

b. The Atlantic connection

The rotated principal component that exhibits the second highest correlation (-0.33) with the GPP index is shown in Fig. 12. This is the leading mode of combined variability and represents the North Atlantic Oscillation (NAO) variability in summer. The SST loadings are confined to the northern basin but the circulation anomalies are well extended both westward (up to and beyond the Great Plains) and eastward. The combined pattern compares favorably with the second-leading pattern in Lanzante's warm season analysis (1984; Fig. 4b). There is little evidence, however, of any trends in the PC distribution, quite unlike the case in winter when the NAO PC exhibits an upward trend since, at least, the early 1970s (Hurrell 1995; Figs. 9a and 12 of Nigam 2003). The warm season PC is, in fact, dominated by intraseasonal variability as its sign changes in 30 of the 49 summers. The contemporaneous correlation with NOAA/CPC's NAO index (see online at <http://www.cpc.ncep.noaa.gov/data/teledoc/nao.html>) in June and July is ~ 0.85 .

The moisture fluxes associated with this mode are shown in the Fig. 12a; the vertically integrated fluxes over the United States are dominated by the stationary component in the lower troposphere. The westward fluxes across the eastern United States track the southern flank of the zonally extended ridge in Fig. 12a. This entire feature, including its North American center, exhibits vertical coherence and thus represents a northward shift of the Bermuda high. Examination of the level-by-level fluxes (not shown) indicates significant interaction with North American orography, which

splits the westward fluxes in the lower troposphere into northwestward and southwestward streams; the latter being stronger. Interestingly, there is little hint of a trough over the Gulf of Mexico in Fig. 12a. The southward fluxes over the southern-tier states, of course, oppose the climatological low-level jet that transports phenomenal amounts of moisture northward from the Gulf of Mexico. The limited impact of this mode on Great Plains precipitation ($\sim 11\%$ of the monthly summer variance) is somewhat surprising in view of its large-scale, coherent structure.

The PC is strongly positive in at least two of the three months during the 1955, 1964, 1967, 1972, 1976, 1983, 1990, and 1994 summers. Comparisons with Fig. 3a indicates that three of these eight summers (1955, 1976, and 1983) were, in fact, dry over the Great Plains. The agreement with observations is even better when the PC is strongly negative (1958, 1993, and 1998)—all three being wet summers.

6. Concluding remarks

The study has sought to ascertain the structure of warm season hydroclimate *variability* over the U.S. Great Plains—a region of profound importance for U.S. agriculture—and the extent to which the observed variability features are represented in the state-of-the-art climate simulations. Interannual variability is the focus here because its spatiotemporal structure is known with less certainty than the seasonal cycle's in both climate observations and simulations. Analysis of interannual variability is thus more exciting and, perhaps, also more important in context of model assessments since model simulations are less scripted in the interannual range; models are typically tuned using observed seasonal variability. The analysis is confined to the latter half of the twentieth century (1950–98) for reasons of circulation data availability, and as such excludes the devastating dust bowl years (1930s). The analyzed period however does include other notable, but shorter duration, dry (1952–55, 1976, 1983–84, 1988, 1992) and wet (1951, 1981, 1993, 1998) summer spells.

The analysis strategy is precipitation centric, and revolves around the Great Plains precipitation index. Unlike previous studies, the GPP index is objectively constructed on the basis of the standard deviation distribution of monthly precipitation in the warm season months (section 3). The index derived from the U.S.–Mexico station precipitation dataset is taken to be the “gold standard,” and its structure and regressions are the target for NCAR and NASA AMIP simulations, and also NCEP and ERA-40 reanalyses. Hydroclimate variability in the reanalyses is not assured to be realistic as the reanalysis procedure is constrained by circulation

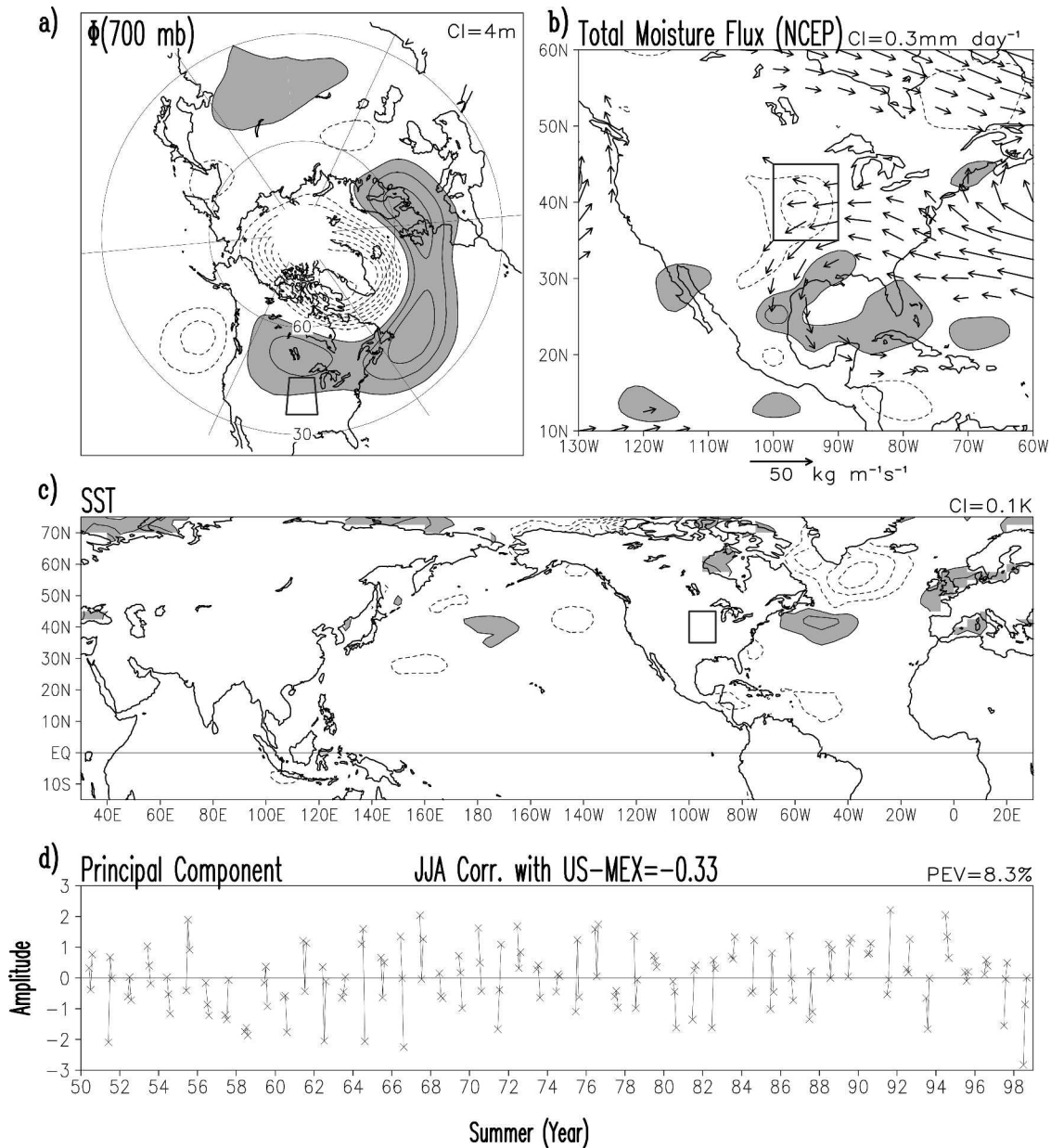


FIG. 12. The Atlantic connection (NAO variability in summer). (d) The rotated PC that exhibits the second highest correlations with the Great Plains precipitation index (U.S.–Mexico station database); the correlation is -0.33 . This is the first PC in a ranking based on explained variance (8.3%). As in Fig. 11, (a) geopotential loadings and (c) SST loadings. (b) The PC regressions on the total (stationary + transient) NCEP moisture flux and its convergence. Contouring and shading as in Fig. 11.

and temperature observations, but not by precipitation and evaporation.

The present analysis is notable also for its investigation of atmospheric water balance over the Great Plains. Although the lack of reliable evaporation estimates preclude definitive assessments, two recent diagnoses enable characterization of the evaporation contribution in Great Plains precipitation variability in reanalysis and simulation datasets.

Interest in low-frequency variability and potential predictability of the Great Plains climate lead to investigation of its linkage with adjoining basin SSTs. Generic concerns associated with the use of indices motivated an objective extraction of the recurrent patterns of combined SST and 700-hPa geopotential variability in the warm season months. The analysis yields a separation of the Pacific and Atlantic basin contributions to Great Plains hydroclimate variability and provides

leads for future investigation of the interaction pathways and mechanisms.

The main findings on the structure and nature of warm season *interannual* variability of Great Plains hydroclimate are as follows:

- Precipitation variability in the reanalysis data is quasi realistic: ERA-40 underestimates the variability amplitude while NCEP overestimates it, both by $\sim 25\%$. ERA-40 variations are temporally better correlated with observations (0.71) than NCEP's (0.53); NCEP and ERA-40 indices are correlated at 0.77.
- Models produce a realistic amplitude of precipitation variability. The evolution is problematic, though, with simulated indices being temporally uncorrelated with the observed monthly GPP index: CAM's correlation is 0.11, while NSIPP's is -0.09 .
- Convective and stratiform components of Great Plains precipitation are very unequal in model simulations: The stratiform component is nearly zero in both NSIPP and CAM models, whereas the two components are comparable in the ERA-40 dataset.
- Vertically integrated moisture fluxes linked with Great Plains precipitation variability are broadly similar in the two reanalysis: Stationary fluxes are at least 5 times larger than the transient ones over the Great Plains, but flux convergences differ by only a factor of 2. ERA-40 fluxes (and convergence) are, however, stronger than NCEP's by as much as 50%. The reanalysis differences are even bigger over the Gulf of Mexico and Caribbean Sea where ERA-40 has robust westward fluxes, which track the southern flank of a coherent anticyclonic circulation that pumps moisture northward from the Gulf. Aspects of this flow feature are absent in the NCEP moisture fluxes.
- Moisture fluxes linked with Great Plains precipitation variability are quite realistic in the NSIPP simulation, being closer to ERA-40 than NCEP. CAM fluxes are however more like NCEP's than ERA-40's.
- Moisture flux convergence accounts for nearly all of the Great Plains precipitation anomaly in ERA-40, but not in NCEP reanalysis and model simulations. Convergent fluxes explain less than half of the precipitation signal in the latter.
- Reanalysis evaporation anomalies over the Great Plains are, apparently, as far apart as the two diagnosed estimates. The NCEP anomaly ranges from 0.1 to 0.3 mm day^{-1} —not unlike the GOLD estimates—while the ERA-40 anomaly is not even up to the contouring threshold (0.1 mm day^{-1}), much like the CPC-based estimate.
- Evaporation anomalies linked with Great Plains precipitation variations are phenomenally strong in

model simulations, reaching 1.2 mm day^{-1} . Very large *local* evaporation in the models—up to 4 times larger than the highest observationally constrained estimate (NCEP's)—suggests a very different view of the anomalous atmospheric water budget; one in which local water sources (precipitation recycling) contribute overwhelmingly to precipitation variability. Model evaporation anomalies are clearly outliers.

- Rotated principal component analysis suggests a Pacific link with Great Plains hydroclimate variability, but the linkage mechanism remains to be elucidated; especially, the potential of concurrent/precursor SST anomalies in the central/eastern tropical Pacific. The Atlantic connection, on the other hand, is evidently through NAO's influence on the Bermuda high, and the resulting interaction of circulation with North American orography; all of which serve to modulate the low-level moisture transports from the Gulf of Mexico.

The study suggests the considerable importance of remote water sources (moisture fluxes) in generation of Great Plains hydroclimate variability. Getting the interaction pathways right is presently challenging for models. Regional hydroclimate simulations and predictions will remain unattainable until models realistically represent the connectivity with remote regions, (i.e., teleconnections). Models currently place a premium on local water sources (precipitation recycling) during warm season variability. Rapid recycling of precipitation must, however, require substantial input of energy into the regional land surface. Investigation of this issue, especially, the role of cloudiness, has been initiated in order to improve understanding of the water and energy cycles over the U.S. Great Plains.

Acknowledgments. The authors would like to acknowledge support of NOAA/PACS Grant NA06GP0362, DOE-CCPP Grant DEFG 0201ER63258, and NSIPP Grant NAG512417. We acknowledge helpful discussions with Mathew Barlow, Ernesto Berbery, Paul Dirmeyer, Hugh van den Dool, Renu Joseph, Adam Schlosser, and Siegfried Schubert. Bob Dickinson and Aiguo Dai offered comments and suggestions on improving the manuscript. We thank Marty Hoerling, Glenn White, and an anonymous reviewer for their constructive input. Phil Pegion and Michael Kistler assisted with the NSIPP data extraction.

REFERENCES

- Amador, J., and Coauthors, cited 2004: North American Monsoon Experiment (NAME): Science and implementation plan. NAME Project Science Team. [Available online at <http://www.cpc.ncep.noaa.gov/products/precip/monsoon/>.]
- Barlow, M., S. Nigam, and E. H. Berbery, 1998: Evolution of the North American monsoon system. *J. Climate*, **11**, 2238–2257.
- , —, and —, 2001: ENSO, Pacific decadal variability, and

- U.S. summertime precipitation, drought, and streamflow. *J. Climate*, **14**, 2105–2128.
- Bell, G. D., and J. E. Janowiak, 1995: Atmospheric circulation associated with the Midwest floods of 1993. *Bull. Amer. Meteor. Soc.*, **76**, 681–695.
- Dai, A., 2001: Global precipitation and thunderstorm frequencies. Part I: Seasonal and interannual variations. *J. Climate*, **14**, 1092–1111.
- , and K. E. Trenberth, 2004: The diurnal cycle and its depiction in the Community Climate System Model. *J. Climate*, **17**, 930–951.
- Dirmeyer, P. A., and L. Tan, 2001: A multi-decadal global land-surface dataset of state variables and fluxes. COLA Tech. Rep. 102, 43 pp. [Available from the Center for Ocean–Land–Atmosphere Studies, 4041 Powder Mill Road, MB 302, Calverton, MD 20705.]
- , X. Gao, and T. Oki, 2002: *GSWP-2: The Second Global Soil Wetness Project Science and Implementation Plan*. IGPO Publication Series, Vol. 37, International GEWEX Project Office, 65 pp.
- Gates, W. L., and Coauthors, 1999: An overview of the results of the Atmospheric Model Intercomparison Project (AMIP I). *Bull. Amer. Meteor. Soc.*, **80**, 29–56.
- Heideman, K. F., and J. M. Fritsch, 1988: Forcing mechanisms and other characteristics of significant summertime precipitation. *Wea. Forecasting*, **3**, 115–130.
- Higgins, R., Y. Chen, and A. Douglas, 1999: Interannual variability of the North American warm season precipitation regime. *J. Climate*, **12**, 653–680.
- Hornberger, G. M., and Coauthors, 2001: A plan for a new science initiative on the global water cycle. U.S. Global Change Research Program Report, Washington, DC, 118 pp. [Available online at <http://www.usgcrp.gov/usgcrp/Library/watercycle/wcsrreport2001/default.htm>.]
- Hu, Q., and S. Feng, 2001: Climatic role of the southerly flow from the Gulf of Mexico in interannual variations in summer rainfall in the central United States. *J. Climate*, **14**, 3156–3170.
- Huang, J., H. M. Van den Dool, and K. P. Georgarakos, 1996: Analysis of model-calculated soil moisture over the United States (1931–1993) and applications to long-range temperature forecasts. *J. Climate*, **9**, 1350–1362.
- Hulme, M., cited 1999: Global Monthly Precipitation, 1900–1999 (Hulme). ORNL DAAC dataset. [Available online at <http://www.daac.ornl.gov/>]
- Hurrell, J., 1995: Decadal trends in the North Atlantic Oscillation: Regional temperatures and precipitation. *Science*, **269**, 676–679.
- Janowiak, J. E., A. Gruber, C. R. Kondragunta, R. E. Livezey, and G. J. Huffman, 1998: A comparison of the NCEP–NCAR reanalysis precipitation and the GPCP rain gauge–satellite combined dataset with observational error considerations. *J. Climate*, **11**, 2960–2979.
- Kalnay, E., and Coauthors, 1996: The NCEP/NCAR 40-Year Reanalysis Project. *Bull. Amer. Meteor. Soc.*, **77**, 437–471.
- Koster, R. D., M. J. Suarez, R. W. Higgins, and H. M. Van den Dool, 2003: Observational evidence that soil moisture variations affect precipitation. *Geophys. Res. Lett.*, **30**, 1241, doi:10.1029/2002GL016571.
- Lanzante, J. R., 1984: A rotated eigenanalysis of the correlation between 700 mb heights and sea surface temperatures in the Pacific and Atlantic. *Mon. Wea. Rev.*, **112**, 2270–2280.
- Lau, K.-M., and H. Weng, 2000: Remote forcing of U.S. summertime droughts and floods by the Asian monsoon? *GEWEX News*, **10**, 5–6.
- Liu, A. Z., M. Ting, and H. Wang, 1998: Maintenance of circulation anomalies during the 1988 drought and 1993 floods over the United States. *J. Atmos. Sci.*, **55**, 2810–2832.
- Mo, K. C., J. Noguez-Paegle, and J. Paegle, 1995: Physical mechanisms of the 1993 summer floods. *J. Atmos. Sci.*, **52**, 879–895.
- , —, and W. R. Higgins, 1997: Atmospheric processes associated with summer floods and droughts in the central United States. *J. Climate*, **10**, 3028–3046.
- Namias, J., 1966: Nature and possible causes of the northeastern United States drought during 1962–65. *Mon. Wea. Rev.*, **94**, 543–554.
- , 1983: Some causes of United States drought. *J. Appl. Meteor.*, **22**, 30–39.
- , 1991: Spring and summer 1988 drought over the contiguous United States—Causes and prediction. *J. Climate*, **4**, 54–65.
- Nigam, S., 2003: Teleconnections. *Encyclopedia of Atmospheric Sciences*, J. R. Holton, J. A. Pyle, and J. A. Curry, Eds., Academic Press, 2243–2269.
- , and H.-S. Shen, 1993: Structure of oceanic and atmospheric low-frequency variability over the tropical Pacific and Indian Oceans. Part I: COADS observations. *J. Climate*, **6**, 657–676.
- , M. Barlow, and E. H. Berbery, 1999: Pacific decadal SST variability: Impact on U.S. drought and streamflow. *Eos, Trans. Amer. Geophys. Union*, **80**, 621–625.
- Prohaska, J. T., 1976: A technique for analyzing the linear relationships between two meteorological fields. *Mon. Wea. Rev.*, **104**, 1345–1353.
- Rayner, N. A., E. B. Horton, D. E. Parker, C. K. Folland, and R. B. Hackett, 1996: Version 2.2 of the global sea-ice and sea surface temperature dataset, 1903–1994. Hadley Centre Tech. Note CRTN 74, 21 pp. [Available from Hadley Centre, Met Office, London Road, Bracknell RS12 2SY, United Kingdom.]
- , D. E. Parker, E. B. Horton, C. K. Folland, L. V. Alexander, D. P. Rowell, E. C. Kent, and A. Kaplan, 2003: Global analyses of sea surface temperature, sea ice, and night marine air temperature since the late nineteenth century. *J. Geophys. Res.*, **108**, 4407, doi:10.1029/2002JD002670.
- Reynolds, R. W., N. A. Rayner, T. M. Smith, D. C. Stokes, and W. Wang, 2002: An improved in situ and satellite SST analysis for climate. *J. Climate*, **15**, 1609–1625.
- Ruiz-Barradas, A., J. A. Carton, and S. Nigam, 2000: Structure of interannual-to-decadal climate variability in the tropical Atlantic sector. *J. Climate*, **13**, 3285–3297.
- Schubert, S. D., M. J. Suarez, P. Pegion, R. J. Koster, and J. T. Bacmeister, 2004: Causes of long-term drought in the U.S. Great Plains. *J. Climate*, **17**, 485–503.
- Ting, M., and H. Wang, 1997: Summertime U.S. precipitation variability and its relation to Pacific sea surface temperature. *J. Climate*, **10**, 1853–1873.
- Trenberth, K. E., 1990: Recent observed interdecadal climate changes in the Northern Hemisphere. *Bull. Amer. Meteor. Soc.*, **71**, 988–993.
- , and C. J. Guillemot, 1996: Physical processes involved in the 1988 drought and 1993 floods in North America. *J. Climate*, **9**, 1288–1298.
- , G. W. Branstator, and P. A. Arkin, 1988: Origins of the 1988 North American drought. *Science*, **242**, 1640–1645.
- Wallace, J. M., and D. S. Gutzler, 1981: Teleconnections in the geopotential height field during the Northern Hemisphere winter. *Mon. Wea. Rev.*, **109**, 784–812.
- Xie, P., and P. A. Arkin, 1997: Global precipitation: A 17-year monthly analysis based on gauge observations, satellite estimates, and numerical model outputs. *Bull. Amer. Meteor. Soc.*, **78**, 2539–2558.
- Xie, S.-P., and Y. Tanimoto, 1998: A pan-Atlantic decadal climate oscillation. *Geophys. Res. Lett.*, **25**, 2185–2188.
- Xue, Y., P. J. Sellers, J. L. Kinter, and J. Shukla, 1991: A simplified biosphere model for global climate studies. *J. Climate*, **4**, 345–364.